# Secondary electron emission in the scanning electron microscope[a)]

H. Seiler
*Institut für Physik der Universität Hohenheim, D-7000 Stuttgart-70, Garbenstr. 30, West Germany*

(Received 7 January 1983; accepted for publication 15 July 1983)

This paper surveys experimental results concerned with secondary electron emission of surfaces bombarded by primary electrons with respect to scanning electron microscopy. The energy distribution, the angular distribution, and the yield of secondary electrons from metals and insulators are reviewed as well as the escape depth of the secondary electrons and the contribution of the backscattered electrons to the secondary electron yield. The different detectors for secondary electrons in the scanning electron microscope are described. The contrast mechanisms in the scanning electron microscope, material, topography, voltage, magnetic, and crystallographic orientation contrast based on secondary electron emission, as well as the lateral resolution, depending among other things on the spatial distribution of the emitted secondary electrons, are discussed.

PACS numbers: 79.20.Hx, 07.80. + x

Introduction
I. Experimental data on secondary electron (SE) emission
  A. Energy distribution of SE
  B. Angular distribution of SE
  C. SE yield of metals and insulators
  D. Escape depth of SE
  E. SE yield as a function of the angle of incidence
  F. Contribution of the backscattered electrons to the SE yield
  G. SE emission on the exit surface of thin transparent films
  H. Noise in SE emission
  I. Exit area of excited SE
  J. Influence of very thin surface layers on SE emission
  K. Semiempiric theory of SE emission
II. Secondary electrons in the scanning electron microscope
  A. SE detectors in the SEM
  B. SE signal in the SEM
  C. Changes of SE emission with time
  D. Contrast in the SEM
    1. Material contrast
    2. Topography contrast
    3. Voltage contrast
    4. Magnetic contrast
    5. Electron channeling and crystallographic contrast
  E. Information depth in the SEM using SE
  F. Lateral resolution in the SEM
  G. Conditions for high resolution in the SEM

## INTRODUCTION

For imaging of surfaces in the scanning electron microscope (SEM) mostly the "true" or slow secondary electrons (SE) are used. These are electrons which leave the surface with energies $E_{SE} \leqslant 50$ eV when the object is bombarded with primary electrons (PE). The SE yield depends on the material and the topography of the specimen. The SE can be deflected and accelerated towards a detector with weak electric fields which do not disturb the energetic primary electron beam. In the SEM we get a strong SE signal with nearly all emitted SE and information on material and topography of the object in fine spot sizes. The SE have only mean escape depths of about $\lambda \approx 1$ nm from metals and so the SE emission is influenced by very thin surface layers. In the SEM, the collector is sensitive not only to SE from the specimen, but also to SE excited by backscattered primaries from inside the specimen chamber. The observed image contrast will depend on several interrelated effects.

Figure 1 shows an arrangement for measuring the SE emission (SEE). The uniform and polycrystalline object is in ultrahigh vacuum (UHV) and the surface is carefully cleaned

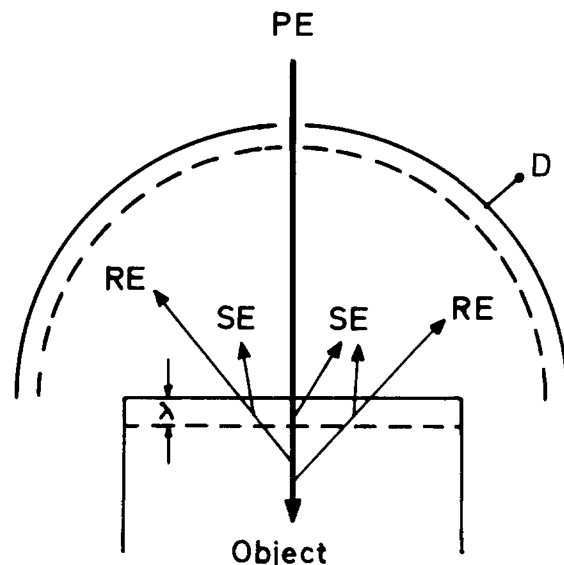


FIG. 1. Arrangement for measuring the SE emission. The secondary electrons (SE) are released by primary electrons (PE) and by backscattered or reflected electrons (RE). The mean escape depth $\lambda$ of the SE is about $\lambda \approx 1$ nm from metals. With the detector $D$ all emitted electrons or only the RE can be measured.

[a)] Dedicated to Professor Dr. Gerhard Pfefferkorn on the occasion on his 70th birthday.



Downloaded 28 Jan 2009 to 146.137.148.78. Redistribution subject to AIP license or copyright; see http://jap.aip.org/jap/copyright.jsp

by several methods. The specimen is bombarded with primary electrons (PE). All emitted electrons independent of their emission direction are collected. It is possible to separate the slow from the energetic backscattered or reflected electrons (RE) by a retarding field. The grid is held negative with respect to the collector so that secondaries formed at the collector do not disturb the measurements. The slow SE are not only released by PE at the entry point but also by RE at the exit point from the specimen.

Figure 2 shows the specimen chamber of a SEM. The sample has a rough surface and underlying object details (such as A and B in Fig. 2) of different material or different crystallographic grains provide image contrasts. Although the escape depth of the SE is very small, object details deeper than the escape depth influence the SE emission and are visible in SEM because the RE also excite SE. The object is normally not in UHV and absorbed layers may be at the surface. So by bombarding the specimen with a PE beam with a high curent density contamination or desorption of the absorbed layers may occur. Both effects may influence the SE emission depending on bombarding time. The SE are extracted by electric fields to one or several detectors. The image contrast from rough surfaces can be improved if the strength of the electric field is insufficient to collect emitted SE. The signal at the detector contains different contributions as shown in Fig. 2.

SE emission has been reviewed by Bruining (1954), Kollath (1956), Ardenne (1956), Jonker (1957), Dekker (1958), Hachenberg and Brauer (1959), Whetten (1961), and Bronshtein and Fraiman (1969). Experimental and theoretical work is described by Kanter (1961), Jahrreiss (1965), Wittry (1966), Mayer and Hölzl (1966), Seiler (1967, 1968a), Appelt (1968), Simon and William (1968), Seah (1969), Drescher *et al.* (1970), Shimizu and Murata (1971), Kanaya and Kawakatsu (1972), Murata (1973), Shimizu (1974), Fitting (1974, 1980), Willis and Feuerbach (1975), Voreades (1976), Pillon *et al.* (1976), Chung and Everhart (1977), Reimer and Drescher (1977), Kanaya and Ono (1978), Alig and Bloom (1978), Ono and Kanaya (1979), Ganachaud and Cailler (1979), Chase *et al.* (1980), Rösler and Brauer (1981), Cailler *et al.* (1981), Seiler (1982), and Halbritter (1982). There exist many books on scanning electron microscopy. In all of them there is at least one chapter which deals with SEE and contrast formation (Thornton 1968; Seiler 1968b; Oatley 1972; Holt *et al.* 1974; Wells 1974; Goldstein and Yakowitz 1975; Reimer and Pfefferkorn 1977). Well known are also "Proceedings of the annual SEM Symposia" (edited by O. Johari) and the "Beiträge zur elektronmikroskopichen Direktabbildung von Oberflächen, BEDO" (edited by G. Pfefferkorn), and some journals with many articles on SEM as "Scanning," "Optik," "Ultramicroscopy" and others. Articles in this journal by Oatley (1982) Niedrig (1982), Joy *et al.* (1982), and Leamy (1982) give information on SE in the SEM.

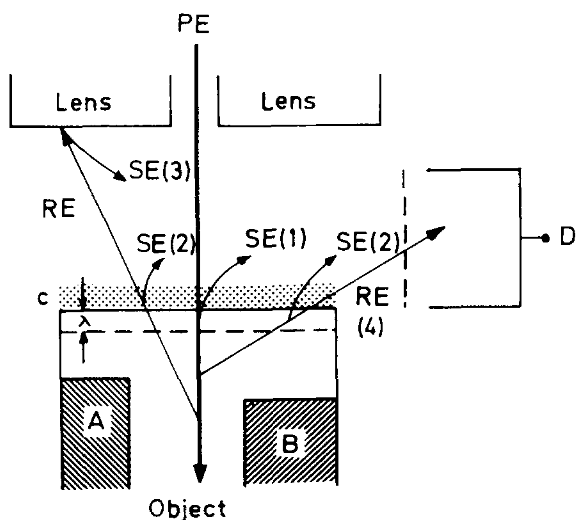


FIG. 2. Measurement of the SE signal in SEM. The surface may be contaminated with layer *C*. The object is not homogeneous. Within the range of the PE and the escape depth of the RE are object details *A* and *B*. The signal of the detector *D* is composed by SE (1): SE released by PE; SE (2): SE released by RE on the object surface; SE (3) released by RE at the walls of the SEM and RE (4) which are emitted in the direction to the detector.

## I. EXPERIMENTAL DATA ON SE EMISSION

If a surface is bombarded with primary electrons (PE), electrons are released.

Figure 3 shows schematically the energy distribution of these electrons released by PE with energies 100 eV $< E_{\rm PE}$ $< 1$ keV. With increasing energy of the PE the elastic peak decreases and a broader maximum of inelastic RE is to be seen. According to their energy the electrons can be divided in different groups:

(1) Electrons with energies $E \leqslant 50$ eV: Secondary electrons (SE);

(2) Electrons with energies 50 eV $< E \leqslant E_{\rm PE}$: Inelastically backscattered and elastically reflected electrons (RE).

According to the different groups we can define

(1) SE-yield $\delta$: number of SE/number of PE;

(2) Backscattering coefficient $\eta$: number of RE/number of PE;

(3) Total electron yield $\sigma = \delta + \eta$;

(4) Coefficient of elastically reflected electrons $\eta_E$: number of elastically reflected electrons/number of PE (Schmid *et al.* 1983).

Superimposed on the energy distribution there are often some peaks. Some of these are Auger electrons (having an

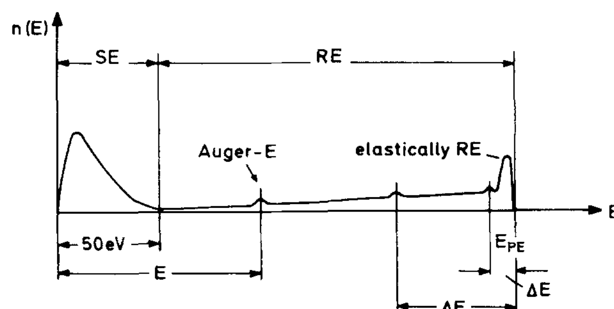


FIG. 3. Schematic energy distribution of electrons which are emitted from a surface bombarded with PE. The SE yield is up to $10^4$ times higher than the Auger electron yield.



Downloaded 28 Jan 2009 to 146.137.148.78. Redistribution subject to AIP license or copyright; see http://jap.aip.org/jap/copyright.jsp

energy depending on the surface material) and others are electrons which are backscattered with an energy loss by volume or surface plasmon excitation or ionization of surface atoms.

### A. Energy distribution of SE

The energy distribution of SE, released by PE with energies more than 100 eV is essentially independent of the energy of the PE, and is characterized by the most probable energy $E^m_{SE}$ and the full width at half maximum (HW). Ideally $E^m_{SE}$ should be measured relative to the Fermi energy level. Both $E^m_{SE}$ and HW depend on the surface material. HW is smaller for insulators than for metals and depends strongly on very thin surface layers (Dietrich and Seiler 1960). According to Kollath (1956), for metals one gets $1.3\ \text{eV} \leqslant E^m_{SE} \leqslant 2.5\ \text{eV}$ and $4\ \text{eV} \leqslant \text{HW} \leqslant 7\ \text{eV}$. New measurements on clean metal surfaces show $1\ \text{eV} \leqslant E^m_{SE} \leqslant 5\ \text{eV}$ and $3\ \text{eV} \leqslant \text{HW} \leqslant 15\ \text{eV}$ (Schäfer and Hölzl 1972). Figure 4 shows typical energy distributions for metals and insulators. (Bouchard and Carette 1980).

According to Chung and Everhart (1974) the shape of the energy distribution of SE is given by

$$\frac{dN}{dE} = k\cdot(E - E_F - \Phi)/(E - E_F)^4, \tag{1}$$

where $k$ is the material constant, $E_F$ is the Fermi energy, and $\Phi$ is the work function.

### B. Angular distribution of SE

The angular distribution (see Fig. 5) of SE from polycrystalline surfaces is a cosine distribution independent of the angle of incidence of the PE (Jonker 1957; Kanaya and Kawakatsu 1972). The angular distribution of SE of a single crystal face shows anisotropy (Burns 1960; Begrambekov *et al.* 1971) and the energy-angle distribution shows a sharp fine structure (Appelt 1968).

### C. SE yield of metals and insulators

Figure 6 shows schematically the SE yield as a function of primary energy $E_{PE}$. The general shape is the same for all materials: $\delta$ increases with $E_{PE}$, reaches a maximum value

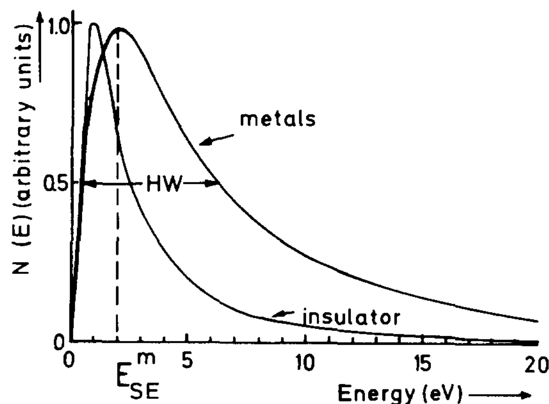


FIG. 4. Energy distribution of SE from metal and insulator surfaces.

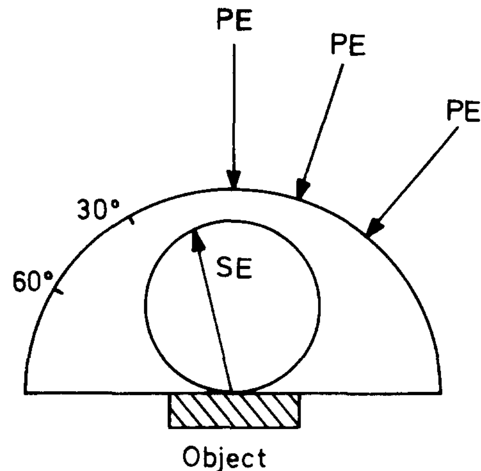


FIG. 5. Angular distribution of SE emitted from a polycrystaline surface.

$\delta^m$ at $E^m_{PE}$ and then decreases with increasing $E_{PE}$. Table I shows values for $\delta^m$ and $E^m_{PE}$ at normal incidence (Seiler 1967, 1968a; Kanaya and Kawakatsu 1972; Kanaya *et al.* 1978; Ono and Kanaya 1979). For the values of the backscattering coefficient $\eta$ at $E^m_{PE}$ see Seiler (1967). For $E_{PE} > 10$ keV, $\eta$ is constant and increases monotonically with the atomic number Z (Ono and Kanaya 1979). This value is shown in Table I. The values $\delta$ (20 keV) were calculated using the semiemperical theory of SEE with formula (16). The values are too high compared with experimental values. According to the measurements of Reimer *et al.* (1968), Seiler (1968a), we get for Al: $\delta$ (20 keV) 0.1–0.17 and for Cu: $\delta$ (20 keV): 0.14. However there are only few measurements available for PE energies used in SEM, so the calculated values are given in Table I.

Some care must be taken comparing the values for $\delta^m$ of different authors because often the maximum total yield $\sigma^m$ is given instead $\delta^m$. The values for $\delta^m$ lie between 0.35 and 1.6 for metals at $100\ \text{eV} \leqslant E^m_{PE} \leqslant 800\ \text{eV}$ and between 1.0 and 10 for insulators at $300\ \text{eV} \leqslant E^m_{PE} \leqslant 2000\ \text{eV}$. High values for $\delta$ are found on single crystals of insulators such as MgO: $\delta^m \approx 20$–25. $\delta^m$ reaches high values if $E^m_{PE}$ is also high. For metals we get $\delta^m/E^m_{PE} \approx 2\times10^{-3}$/eV (Ono and Kanaya 1979). An example for the simultaneous increase of $\delta^m$ and $E^m_{PE}$ was shown by Beisswenger and Gruner (1974) at reactive evaporated BeO layers. There exists no simple relation

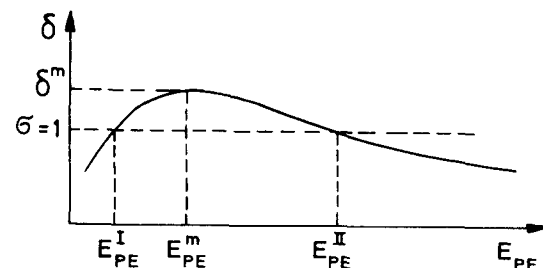


FIG. 6. SE yield $\delta$ depending on $E_{PE}$.



Downloaded 28 Jan 2009 to 146.137.148.78. Redistribution subject to AIP license or copyright; see http://jap.aip.org/jap/copyright.jsp

TABLE I. $\delta^m$ maximum of the SE yield for different atomic numbers $Z$ and calculated values for $\delta$ and $\eta$ for typical energies used in the SEM.

| $Z$ | Atom | $\delta^m$ | $E_{PE}^m$(eV) | $\eta$ ($E_{PE} > 10$keV) | $\delta$(20 keV) calc. |
|---|---|---|---|---|---|
| 3 | Li | 0.5–0.6 | 100–200 | 0.07 | 0.13 |
| 4 | Be | 0.5–0.9 | 200–300 | 0.08 | 0.18 |
| 5 | B | 1.0–1.2 | 150–400 | 0.08 | 0.34 |
| 6 | C | 0.9–1.0 | 300–1100 | 0.1 | 0.28 |
| 11 | Na | 0.65 | 300 | 0.19 | 0.17 |
| 12 | Mg | 0.8–0.9 | 300 | 0.2 | 0.24 |
| 13 | Al | 0.9–1.0 | 250–300 | 0.2 | 0.28 |
| 14 | Si | 0.9–1.1 | 250–300 | 0.22 | 0.30 |
| 15 | P | (1.2) | (550) | 0.23 | 0.38 |
| 16 | S | (1.2) | (560) | 0.25 | 0.38 |
| 19 | K | 0.5–0.7 | 300 | 0.28 | 0.15 |
| 20 | Ca | (0.85) | (390) | 0.28 | 0.24 |
| 21 | Sc | 0.8 | 300 | 0.29 | 0.22 |
| 22 | Ti | 0.7–0.9 | 300 | 0.3 | 0.22 |
| 23 | V | (1.0) | (470) | 0.31 | 0.30 |
| 24 | Cr | (1.0) | (480) | 0.32 | 0.30 |
| 25 | Mn | (1.0) | (500) | 0.32 | 0.30 |
| 26 | Fe | 1.1–1.3 | 400 | 0.33 | 0.38 |
| 27 | Co | 0.9–1.2 | 400–600 | 0.33 | 0.32 |
| 28 | Ni | 1.0–1.3 | 500–550 | 0.34 | 0.37 |
| 29 | Cu | 1.1–1.3 | 500–600 | 0.34 | 0.38 |
| 30 | Zn | 0.9–1.1 | 200–500 | 0.35 | 0.30 |
| 31 | Ga | 1.3 | 300–500 | 0.35 | 0.42 |
| 32 | Ge | 1.0–1.2 | 300–500 | 0.35 | 0.34 |
| 33 | As | (1.4) | (670) | 0.36 | 0.47 |
| 34 | Se | 0.6–1.3 | 400–500 | 0.36 | 0.28 |
| 37 | Rb | 0.6–0.9 | 350–400 | 0.37 | 0.20 |
| 38 | Sr | 0.8 | 250 | 0.37 | 0.22 |
| 39 | Y | 0.8 | 350–400 | 0.38 | 0.22 |
| 40 | Zr | 0.9–1.1 | 350 | 0.38 | 0.30 |
| 41 | Nb | 1.1–1.2 | 550 | 0.38 | 0.36 |
| 42 | Mo | 1.0–1.2 | 400 | 0.38 | 0.34 |
| 43 | Tc | (1.1) | (560) | 0.38 | 0.34 |
| 44 | Ru | (1.1) | (580) | 0.39 | 0.34 |
| 45 | Rh | (1.1) | (580) | 0.39 | 0.34 |
| 46 | Pd | 1.3 | 650 | 0.39 | 0.42 |
| 47 | Ag | 1.2–1.4 | 700–800 | 0.39 | 0.42 |
| 48 | Cd | 0.9–1.1 | 400–500 | 0.4 | 0.3 |
| 49 | In | 1.3–1.4 | 500 | 0.4 | 0.45 |
| 50 | Sn | 1.1–1.4 | 500 | 0.4 | 0.40 |
| 51 | Sb | 1.2–1.3 | 600 | 0.4 | 0.40 |
| 52 | Te | 1.4 | 700 | 0.41 | 0.47 |
| 55 | Cs | 0.5–0.8 | 300–400 | 0.41 | 0.17 |
| 56 | Ba | 0.7–0.9 | 400 | 0.41 | 0.22 |
| 57 | La | 0.8 | 500 | 0.41 | 0.22 |
| 58 | Ce | (0.6) | (240) | 0.41 | 0.15 |
| 72 | Hf | 1.1 | 460 | 0.43 | 0.34 |
| 73 | Ta | 1.0–1.35 | 600 | 0.43 | 0.37 |
| 74 | W | 1.0–1.4 | 700 | 0.43 | 0.38 |
| 75 | Re | 1.3 | 900 | 0.43 | 0.42 |
| 76 | Os | 1.3 | (730) | 0.43 | 0.42 |
| 77 | Ir | (1.5) | (770) | 0.43 | 0.52 |
| 78 | Pt | 1.35–1.7 | 700–750 | 0.43 | 0.52 |
| 79 | Au | 1.2–1.6 | 700–875 | 0.45 | 0.47 |
| 80 | Hg | 0.9–1.1 | 600 | 0.45 | 0.30 |
| 81 | Tl | 1.4 | 650 | 0.45 | 0.47 |
| 82 | Pb | 1.0–1.3 | 500–700 | 0.45 | 0.37 |
| 83 | Bi | 1.2–1.3 | 500–700 | 0.45 | 0.40 |
| 90 | Th | 0.9–1.3 | 600–800 | 0.45 | 0.34 |

between $\delta$ and the atomic number $Z$ of the surface atoms, so material analysis by measuring the SE yield is not possible. Many authors tried to show relations between the dependence of $\delta^m$ and regularities of the elements of the periodic table (e.g., Seiler 1967; Ono and Kanaya 1979; Makarov and Petrov 1981). Materials consisting of atoms with a large diameter have small $\delta^m$ (Seiler 1967). According to Ono and Kanaya (1979), $\delta^m$ and $E_{PE}^m$ depend both on the ionization energy $J$ of the surface atoms: $\delta^m \sim J^{4/5}$, $E_{PE}^m \sim J^{4/5}$.

A survey on some measured values of $E_I < E_{PE}^m$ and $E_{II} > E_{PE}^m$ for which $\delta = 1$ at some metal surfaces are given by Whetten (1961):

Ag: $E_I = 200$ eV, $E_{II} > 2000$ eV;
Au: $E_I = 300$ eV, $E_{II} > 2000$ eV;
Pt: $E_I = 350$ eV, $E_{II} = 3000$ eV;
Si: $E_I = 125$ eV, $E_{II} = 500$ eV;
Cu: $E_I = 200$ eV, $E_{II} = 1500$ eV.

Table II shows some values of $\sigma^m$ and $E_{PE}^m$ for compounds and insulators. Measurements of the SEE of insulators are difficult to make because of charging effects. For the investigation of insulators and electrical floating objects the values of $E_{PE}$ where $\sigma = 1$ are important (See $E_{PE}^{I}$ and $E_{PE}^{II}$ in Fig. 6). Using these PE energies the potential of the surface will stabilize. For $E_{PE} > E_{PE}^{II}$ as normally used in the SEM, the potential of the surface becomes negative because $\sigma < 1$; more electrons reach the surface than SE and RE leave the surface. The PE are decelerated, thus increasing $\sigma$ until $\sigma = 1$. The negative potential of the surface can reach very high values up to the potential of the electron gun. For $E_{PE}^{I} < E_{PE} < E_{PE}^{II}$ the sample becomes positively charged because $\sigma > 1$. The PE are accelerated until $\sigma = 1$ is reached and so the crossover for $E_{PE}^{II}$ gives a stable point. The positive potential however can only reach values of the collector potential, otherwise the SE will return to the surface.

The SE yield of thin insulating layers on a conducting bulk material increases by positive charging of the surface. If

TABLE II. $\sigma^m$ maximum of the total SE yield of some compounds and insulators according to Whetten (1961).

| | $\sigma^m$ | $E_{PE}^m$ |
|---|---|---|
| $Cu_2O$ | 1.2 | 400 |
| PbS | 1.2 | 500 |
| $Ag_2O$ | 1.0–1.2 | 500 |
| $MoO_2$ | 1.1–1.3 | 450 |
| CsCl | 6.5 | ... |
| $Al_2O_3$ | 2.6–4.7 | 600 |
| $SiO_2$ | 2.1–2.9 | 400 |
| ZnS | 1.8 | 350 |
| Mica | 2.4 | 350 |
| Glass | 2–3 | 300–450 |
| $BaF_2$ | 4.5 | ... |
| $SbCs_3$ | 6 | 700 |
| GeCs | 7 | 700 |
| BeO | 3.4–10 | 400–2000 |
| BaO | 2.3–4.8 | 400 |
| CaO | 2.2 | 500 |
| KBr (crystal) | 14 | 1800 |
| (layer) | 7.5 | 1600 |
| NaBr (crystal) | 24 | 1800 |
| (layer) | 6.3 | ... |
| NaCl (crystal) | 14 | 1200 |
| (layer) | 6.5 | 600 |
| KCl (crystal) | 12 | 1600 |
| (layer) | 7.5 | 1200 |



Downloaded 28 Jan 2009 to 146.137.148.78. Redistribution subject to AIP license or copyright; see http://jap.aip.org/jap/copyright.jsp

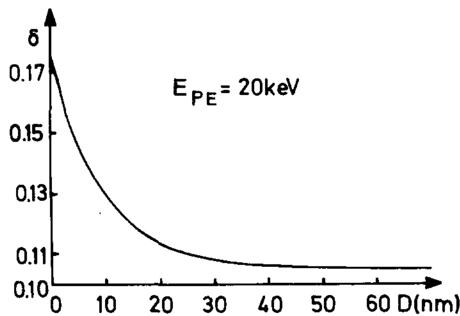


FIG. 7. Decrease of $\delta$ of an aluminum surface at $E_{PE} = 20$ keV depending on the thickness of a contamination layer grown under electron bombardment.

the electric field strength within the layer exceeds $10^7$ V/cm the Malter (1936) effect sets in, i.e., the electron emission is caused by field emission at the bulk material through the insulating layer. In this case the electron yield becomes independent of the PE current. In the case of the field enhanced SEE the electric field is less than $10^7$ V/cm, so no field emission can occur—however, the escape possibility of the SE is increased. Seiler (1967) estimated that on thin insulating layers an increase of the yield by about 4–5 is possible. Very high SE yields ($\delta > 20$) are found on low density layers of KCl, $BaF_2$, (Goetze *et al.* 1964; Goetze 1968; Seiler and Stärk 1965a).

In the SEM the energies of the PE are normally higher than $E^m_{PE}$. From $E_{PE} = 10$ to 100 keV, $\delta$ decreases with $E_{PE}^{-0.8}$ (Reimer *et al.* 1968). For Al, $\delta$ decreases from $\delta \approx 0.3$ ($E_{PE} = 10$ keV) to $\delta \approx 0.03$ ($E_{PE} = 100$ keV). Furthermore the SE yield in a SEM with a normal high vacuum is influenced by the growth of a contamination layer at the impact point of the electron beam (Wittry 1966; Seiler 1967). Figure 7 shows the way in which the SE yield of an Al surface decreases with bombarding time.

### D. Escape depth of SE

Only SE excited near the surface can reach and escape from the surface (Copeland 1940). Normally it is assumed that the escape probability for SE produced at a distance $x$ from the surface, decreases with $e^{-x/\lambda}$, where $\lambda$ is the mean escape depth. Some measurements give the maximum escape depth $T$, other the mean escape depth $\lambda$ (Seiler 1967). Layers of increasing thickness were produced on a bulk substrate [see Fig. 7 (Seiler and Stärk 1965b)]. Beyond the particular thickness $T$ of the layer, $\delta$ no longer depends on the underlaying bulk material. If $\eta_{\text{bulk}} = \eta_{\text{layer}}$, $T$ gives a maximum escape depth of the SE and we can assume that $T \approx 5\lambda$ (Seiler 1967). The escape depth of the SE from metals is of the order of $\lambda \approx 0.5$–$1.5$ nm, $T \approx 5$ nm; of insulators of $\lambda \approx 10$–$20$ nm, $T \approx 75$ nm. Mean escape depths of metallic oxides as $Al_2O_3$ and MgO and alkali halides as $BaF_2$, NaCl, and KCl are calculated by Kanaya *et al.* (1978). The high SE yield of insulators can be explained by the large escape depths of the SE. According to calculations by Ono and Kanaya (1979) the escape depth of SE can be correlated with regularities of the elements of the periodic table.

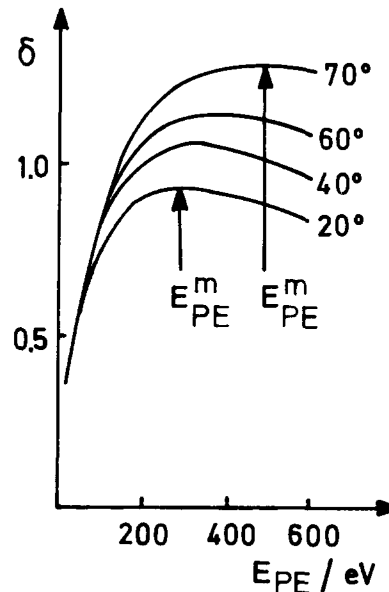


FIG. 8. Dependence of $\delta$ on the energy of the PE for different angle of incidence.

### E. SE yield as a function of the angle of incidence

$\delta$ increases with increasing angle of incidence $\vartheta$ measured relative to the surface normal for $\vartheta < 80°$ according to

$$\delta(\vartheta) = \delta_0(\cos\vartheta)^{-n}; \quad \delta_0 = \delta(\vartheta = 0°). \tag{2}$$

The value $n = 1$ is valid for material with about $Z = 30$. For light elements $n$ increases (Bronshtein and Dolinin 1968; Reimer and Pfefferkorn 1977) to about $n \approx 1.3$, and for heavy elements $n$ decreases to about $n \approx 0.8$. Kanaya and Kawakatsu (1972) give values $1.3 \leqslant n \leqslant 1.5$.

The increase of $\delta$ with increasing $\vartheta$ is due to the small escape depth of the SE. The longer the penetration distance of the PE within the escape depth of the SE, the higher the yield. With increasing $\vartheta$, $\delta^m$, $E^m_{PE}$, and $E^{II}_{PE}$ increase (Bruining 1954; Kollath 1956; Reimer and Pfefferkorn 1977; Salehi and Flinn 1981). (See Fig. 8.) Using single crystals there is a fine structure superimposed on the monotonic increase of $\sigma$, $\eta$, and $\delta$ with increasing $\vartheta$ as shown in Fig. 9. This gives the

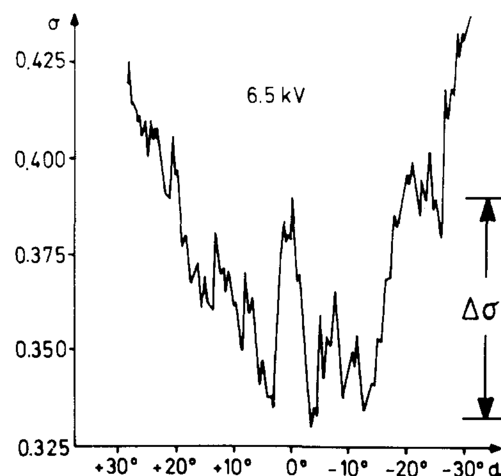


FIG. 9. Dependence of $\sigma = \delta + \eta$ on the angle of incidence for a Si (111) face (Kuhnle and Seiler 1970).



Downloaded 28 Jan 2009 to 146.137.148.78. Redistribution subject to AIP license or copyright; see http://jap.aip.org/jap/copyright.jsp

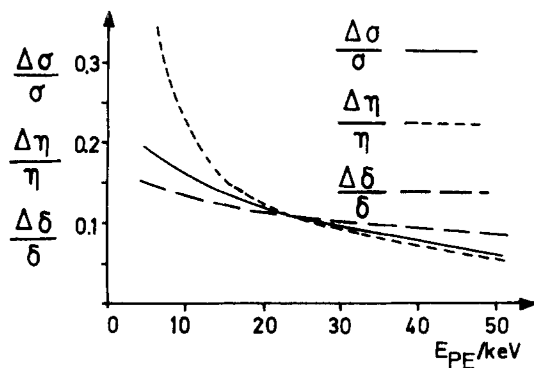


FIG. 10. Dependence of the anisotropy $\Delta\sigma/\sigma$, $\Delta\eta/\eta$, and $\Delta\delta/\delta$ of a Si (111) face on the energy of the Pf (Seiler and Kuhnle 1970).

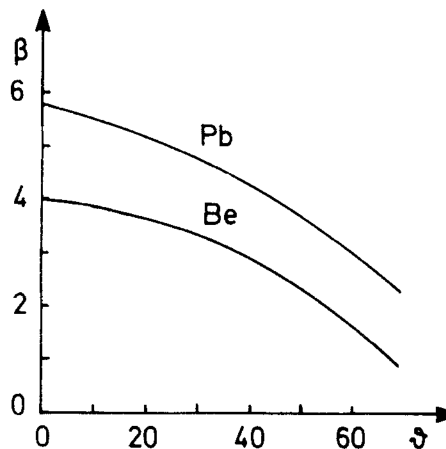


FIG. 11. Decrease of $\beta$ with increasing angle of incidence according to the measurements of Bronshtein (1965, 1967) for $E_{PE} = 4$ keV.

electron channeling pattern (ECP) in the SEM and the crystal orientation contrast in both in the SEM and the electron emission microscope using SE (Carle and Seiler 1966).

Crystallographic contrast effects in the SE, the RE, the Auger electron, and the x-ray yield can be explained by excitation of Bloch waves (Howie 1974). The fine structure of the SE and RE, i.e., the difference in the intensities $\Delta\delta$ and $\Delta\eta$, when changing the angle of incidence from a direction parallel to the lattice plane to the Bragg angle, was measured by a number of authors, e.g., Palmberg (1967). $\Delta\sigma/\sigma$, $\Delta\eta/\eta$, and $\Delta\delta/\delta$ decrease with increasing $E_{PE}$ as shown in Fig. 10 (Seiler and Kuhnle 1970).

### F. Contribution of backscattered electrons to SE yield

SE are not only released by PE but also by RE. This contribution by RE to the SE yield has been investigated by several authors (Everhart 1958; Kanter 1961; Bronshtein and Fraiman 1969; Seiler 1967, 1968a; Drescher *et al.* 1970; Kanaya and Kawaktsu 1972; Fitting *et al.* 1976; Reimer and Drescher 1977; Robinson 1974). The SE yield is given by two parts:

$$\delta = \delta_{PE} + \eta\delta_{RE} = \delta_{PE}(1 + \beta\eta). \quad (3)$$

$\delta_{PE}$ is the number of SE released per PE, $\delta_{RE}$ is the number of SE released per RE, $\beta = \delta_{RE}/\delta_{PE}$. For $E_{PE} > E^{m}_{PE}$ there is a higher probability for a SE to be excited by a RE than by a PE, so that $\beta > 1$. Bronshtein [reviewed by Seiler (1967)] measured $\beta \approx 4$ for $E_{PE} < 5$ keV, Drescher *et al.* (1970) measured $\beta \approx 2$ for $E_{PE} > 10$ keV. There are two reasons why $\beta > 1$. First, the mean energy of the RE is less than $E_{PE}$ and so $\delta$ is nearer to $\delta^m$. Second, the lower average emergence angle of the RE is more favorable for the excitation of SE than the normal incidence of the PE beam.

This contribution of RE to $\delta$ is very important in the SEM. In such a case, where a contamination layer is on the object surface, image contrasts are caused by variation in $\eta$ rather than in $\delta$. For an Al surface with a contamination layer we get a yield $\delta \approx 0.10$ at $E_{PE} = 20$ keV. With $\beta = 2$ we can calculate that $\delta_{PE} = 0.07$ and $\delta_{RE} = 0.14$.

$\beta$ decreases with angle of incidence of the PE. Figure 11 shows the dependence of $\beta$ on the angle of incidence according to the measurements of Bronshtein and Denisov (1967) [surveyed by Seiler (1967)].

Kanter (1961) showed that the SE yield of thin foils is less than that of bulk material. If most PE can penetrate the thin foil, $\eta$ is very small and hence the SE are released almost exclusively by PE. The dependence of $\eta$ on the thickness $D$ of the foil was used by Niedrig and Sieber (1971) to measure $D$. According to Eq. (3) the SE yield $\delta$ depends on $\eta$ and so also on the thickness of the foil.

### G. SE emission on the exit surface of thin transparent films

The SE are not only released on the surface of bulk material and thin foils but also on the back side (bottom) of transparent films if the energy of the PE is great enough (Fig. 12). There are many measurements on SEE in transmission on thin films (Kanter 1961; Jahrreiss 1972; Hasselbach 1975; Reimer and Drescher 1977; Ono and Kanaya 1979; Kadlec and Eckertova 1970; Fitting 1974). On the entrance side the number $\eta\,\delta_{RE}$ of SE released by RE is given by

$$\eta\delta_{RE} = \delta_{PE}\,\beta\,\eta. \quad (4)$$

On the exit side the number $t\,\delta_T$ of SE released by transmitted electrons can be expressed by (Reimer and Drescher 1977)

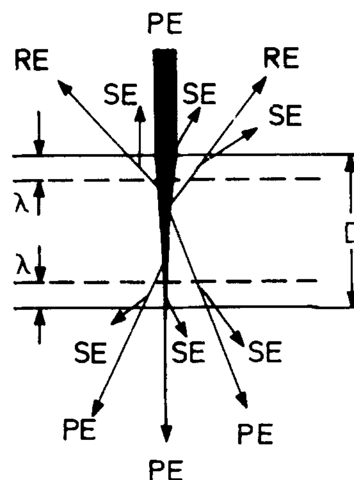


FIG. 12. SE emission of a transparent foil.



Downloaded 28 Jan 2009 to 146.137.148.78. Redistribution subject to AIP license or copyright; see http://jap.aip.org/jap/copyright.jsp

$$t\delta_T = \delta_{PE}\,\beta_t\,t, \text{ with } \beta_t = \delta_T/\delta_{PE}. \quad (5)$$

$t$ is the transmission coefficient, $\delta_T$ is the number of SE/number of transmitted electron.

If the thickness of the foil is an appreciable fraction of the electron penetration depth, then the energy loss of the PE within the foil must be taken into consideration. At the exit side the maximum of the yield is at a higher value of $E_{PE}$ than at the entrance side of the foil. Also the shape of the curve $\delta_T(E_{PE})$ is different from $\delta(E_{PE})$ because of the broadening of the energy distribution of the electrons in the foil. Figures 13 and 14 show the SE yield of Al foils on the entrance and on the exit surface for different energies of the PE as a function of the foil thickness. According to Reimer and Drescher (1977), $\beta_t$ increases with $D/R$, $D$ = thickness of the foil and $R$ = range of the PE. For $D/R = 1$ we get $\beta_t = 3$ for Al and $\beta_t = 2$ for Au. This can be explained similarly as in the case of RE. The transmitted electrons have lower energy than the PE and so their energy is nearer to the energy in the maximum of the SE yield and the angular distribution of the scattered transmitted electrons causes a higher SE yield than that of the PE at normal incidence. There is no experimental evidence that the conservation of momentum causes a higher SE yield in the direction of the PE beam as proposed by Robinson (1975). Within the solid an isotropic distribution of the excited electrons is assumed. Only in insulators with internal electric fields may there occur deviations from isotropic distribution.

### H. Noise in SE emission

The incident PE beam is modulated by "shot noise." The noise in SE emission was investigated by several authors with respect to the SEM: Everhart (1958, 1970), Reimer and Pfefferkorn (1977), Baumann and Reimer (1981). According to Filippov (1966) for $E_{PE} \leqslant 250$ eV the SE emission shows a Poisson distribution. For energies used in the SEM the distribution of the SE yield is more complicated (Kurrelmeyer and Hayner 1937; Everhart *et al.* 1959; Reimer 1971) because the primary electrons and the RE can produce further SE at the surface when leaving the specimen. The distribution is therefore not simply a Poisson distribution but shows an increased relative variance. (Reimer and Pfefferkorn 1977).

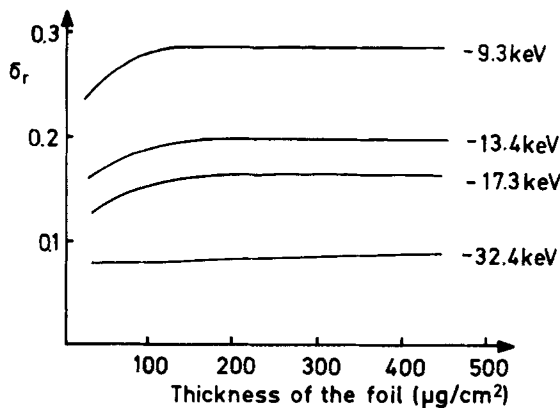


FIG. 13. SE yield $\delta$ at the entrance surface of a thin Al foil depending on the foil thickness for different PE energies according to Reimer and Drescher (1977).

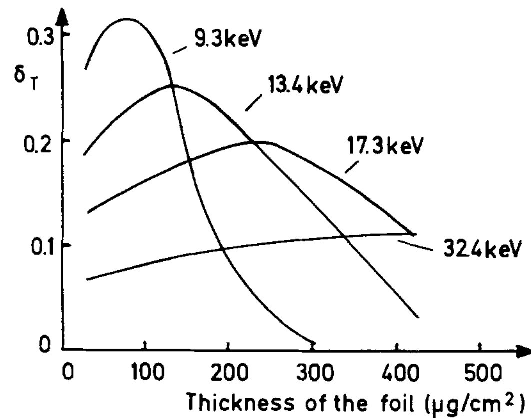


FIG. 14. SE yield $\delta_T$ at the exit surface of a thin Al foil depending on the foil thickness for different PE energies according to Reimer and Drescher (1977).

### I. Exit area of excited SE

The width of the exit area of the primary excited SE is determined by the mean escape depth $\lambda$ of the SE. [See Fig. 15 (a)] (Wells 1957; Everhart 1958; Everhart and Chung 1972). If $d_0$ is the diameter of the incident beam, the exit

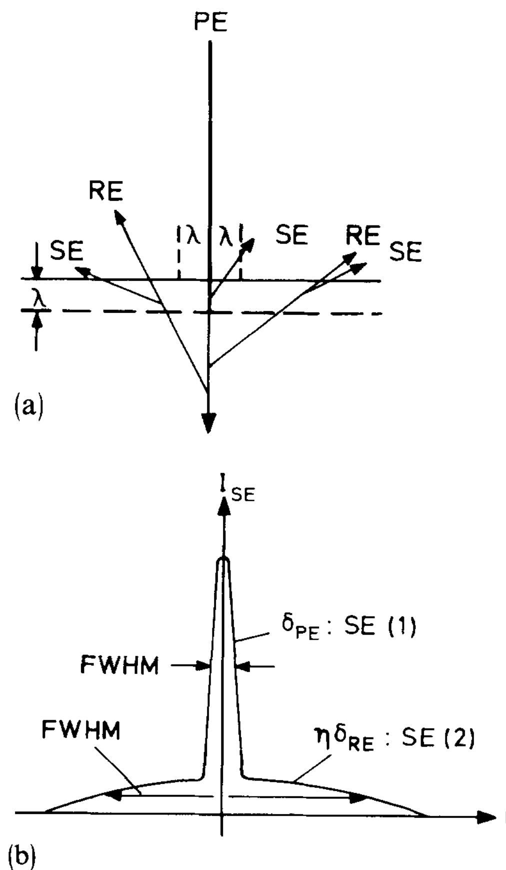


FIG. 15. Spatial distribution of SE released at a surface by PE and by RE. (a) The SE are released by the PE within a circle determined by the mean escape depth of $\lambda$ of the SE. (b) Schematic intensity distribution of the SE (1) signal and SE (2) signal depending on the distance $r$ from the impact of the primary beam. FWHM: Full width at half maximum.



Downloaded 28 Jan 2009 to 146.137.148.78. Redistribution subject to AIP license or copyright; see http://jap.aip.org/jap/copyright.jsp

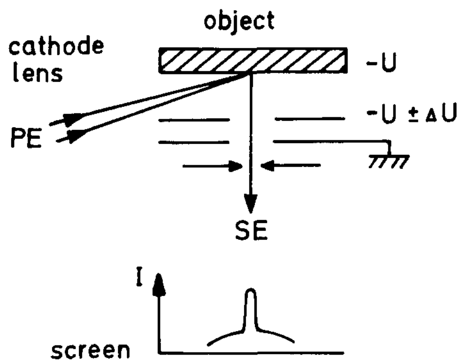


FIG. 16. Arrangement for measuring the spatial distribution of SE released by a fine electron probe (Hasselbach and Rieke 1982).

diameter of the primary excited SE may be estimated by $\sqrt{d_0^2 + \lambda^2}$. The SE excited by the RE will emerge over approximately the same area as the RE. The width of the exit area of these SE is determined by the range of the electrons [see Fig. 15(a)]. The schematic intensity of the both parts of the SE released by PE and by RE is shown in Fig. 15(b). The spatial distribution of SE released by a fine electron probe was measured by Hasselbach (1973), Hasselbach and Rieke (1978, 1982), with a combination of a SEM and an electron emission microscope (EEM). Normally in the EEM (Möllenstedt and Lenz 1963) the whole object surface is stimulated to emit electrons by UV light, heating, or by bombardment with PE or ions. It is possible to image the specimen with the emitted slow electrons by a cathode or immersion lens (see Fig. 16). This is a combination of an electric accelerating field and an electrostatic or magnetic electron lens. By using a cathode lens it is possible to get a picture of the spatial distribution of the SE emitted by a fine PE probe. The RE are prevented from reaching the image plane by an aperture in the focal plane of the cathode lens. According to Hasselbach and Rieke (1982) the spatial distribution of SE released by RE can both be approximated by Gaussian distributions. In

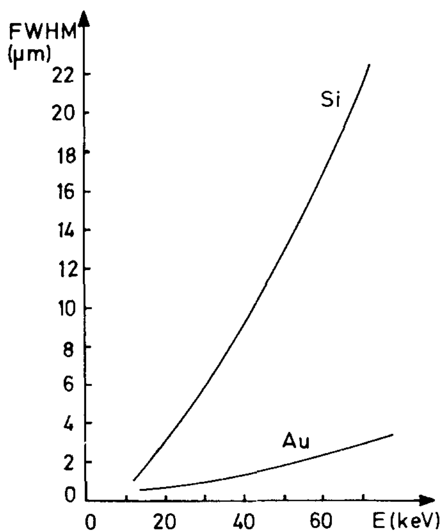


FIG. 17. Full width at half maximum (FWHM) of the SE spatial distribution released by RE depending on the energy of the PE for Si and Au. (Hasselbach and Rieke 1982).

Fig. 17 the full width at half maximum (FWHM) of the density distribution of SE released by RE on Si and Au is shown for energies of the PE from 20–70 keV.

### J. Influence of very thin surface layers on SE emission

The work function $\Phi$ has less effect on SE emission as compared with photo, thermionic- and field-electric emission. Metals with high $\Phi$ often show also high $\delta$. Of the three processes which contribute to SE emission, (1) electron production within the material, (2) migration of the electrons to the surface, and (3) escape of the SE over the surface potential barrier, the first two processes strongly depend on the bulk properties, while the third process should cause an increase in $\delta$ with decreasing $\Phi$. Palmberg (1967), Schäfer and Hölzl (1972) tried to reduce $\Phi$ by evaporating Na on Ge or Pt surfaces. Reduction of $\Phi$ from 4.79 to 2.3 eV increased $\delta^m$ from 1.2 to 3.6, while $E_{\rm PE}^m$ increased from 700 to 2000 eV.

The SE emission can be influenced by resonant tunneling (Grundner and Halbritter 1980; Halbritter 1982, 1983). Thin absorbed layers of $H_2O$ may enhance the SE yield up to 50% whereas the growth of unsaturated polymerized hydrocarbon layer may reduce the SE yield.

### K. Semiempirical theory of SE emission

The elementary theory developed by Salow (1940) and Bruining (1954) has been reviewed by Dekker (1958) and Kollath (1956). The SE yield can be written in the following form:

$$\delta = \int n(x, E_{\rm PE}) f(x) dx. \tag{6}$$

$n(x,E_{\rm PE})$ is the number of SE produced at a distance $x$ from the surface by a PE of the energy $E_{\rm PE}$, $f(x)$ is the probability that a SE produced at $x$ reaches the surface and is emitted into vacuum.

Assuming that $n(x,E_{\rm PE})$ is proportional to the average loss per unit path length

$$n(x,E_{\rm PE}) = -\frac{1}{\epsilon}\frac{dE}{dx}. \tag{7}$$

$\epsilon$ is the energy required to produce a SE. It is generally assumed that

$$f(x) = B\, e^{-x/\lambda}, \tag{8}$$

where $B$ is a constant $< 1$ and takes into account that only a fraction of the excited electrons migrates toward the surface and the probability of these electrons reaching the surface and passing over the surface barrier into vacuum.

According to Young (1956, 1957) the energy dissipation of PE within the material is approximately constant and hence

$$\frac{-dE}{dx} = \frac{E_{\rm PE}}{R}, \tag{9}$$

where $R$ is the range of the PE. From Eqs. (6)–(9) we get an expression for $\delta(E_{\rm PE})$

$$\delta = \int_0^\infty \frac{B}{\epsilon}\frac{E_{\rm PE}}{R} e^{-x/\lambda}\, dx, \tag{10}$$



Downloaded 28 Jan 2009 to 146.137.148.78. Redistribution subject to AIP license or copyright; see http://jap.aip.org/jap/copyright.jsp

$$\delta = B\frac{E_{\rm PE}}{\epsilon}\frac{\lambda}{R}(1 - e^{-R/\lambda}). \tag{11}$$

Using the energy-range relation (Young 1959)

$$\frac{R}{nm} = \frac{1.15\times 10^5}{\rho({\rm kg/m^3})}\left(\frac{E_{\rm PE}}{\rm keV}\right)^{1.35}, \tag{12}$$

we get $\delta = \delta(E_{\rm PE})$ or $\delta = \delta(R)$. $\delta(E_{\rm PE})$ is a function which increases with $E_{\rm PE}$ up to a maximum $\delta^m$ at $E^m_{\rm PE}$ and then decreases.

The reduced yield $\delta/\delta^m$ as a function of $E_{\rm PE}/E^m_{\rm PE}$ is independent of the constants $B,\epsilon,\rho$, which are characteristic for the material under consideration. Thus according to this theory the reduced yield curves should all follow a single universal curve.

$$\frac{\delta}{\delta^m} = 1.11(E_r)^{-0.35}(1 - e^{-2.3E_r^{1.35}}), \tag{13}$$

with $E_r = E_{\rm PE}/E^m_{\rm PE}$.

Calculating the maximum of the yield curve $\delta = \delta(R)$ we get the maximum for

$$R = 2.3\lambda. \tag{14}$$

According to several authors (Seiler 1967; Simon and Williams 1968; Buchholz 1969) the maximum of the yield curve is reached if the range $R$ of the PE is approximately equal to the escape depth of the SE. For values $R$ between maximum and mean escape depth, the theoretical value corresponds well with the experimental data. For $E_{\rm PE} \gg E^m_{\rm PE}$ we get from Eq. (13)

$$\delta = 1.11\,\delta^m(E_r)^{-0.35}. \tag{15}$$

Using the experimental values of Ono and Kanaya (1979)

$$\frac{\delta^m}{E^m_{\rm PE}/{\rm keV}} \approx k, \quad 1.87 \leqslant k \leqslant 2.4,$$

we get for $k = 2.1$

$$\delta = 0.86\,(\delta^m)^{1.35}\left(\frac{E_{\rm PE}}{\rm keV}\right)^{-0.35}. \tag{16}$$

Calculated values of $\delta$ for $E_{\rm PE} = 20$ keV are shown in Table I. Those values are greater than experimental values, but are useful for estimating image contrasts. Seiler (1982) surveyed modern theories of SE emission.

## II. SE IN THE SCANNING ELECTRON MICROSCOPE

In a SEM a fine PE beam is scanned over the specimen. The electron current leaving the surface is amplified and is used to modulate the brightness of a cathode ray tube, whose electron beam is moving over the screen synchronously with the PE beam. Surfaces were imaged using SE in experimental SEM's by Knoll (1935). Knoll and Theile (1939) show magnified images of surfaces with material, topography, and crystallographic contrast. Ardenne (1940) described a SEM for surface imaging. A voltage contrast was observed by Knoll (1941). Smith *et al.* (1955) used a SEM with a resolution better than 50 nm. Oatley and Everhart (1957) examined *p-n* junctions with a SEM.

### A. SE detectors in the SEM

In the SEM the generated SE must be collected and the signal must be amplified without introducing additional noise.

#### *1. Measurement of the sample current*

The sample current $i_s = i_{\rm PE} - i_{\rm SE} - i_{\rm RE}$ can be measured by amplifying the voltage drop on a resistor or with a low noise operational amplifier with high input impedance (Knoll 1935; Oatley 1981). This signal gives, however, a poor $S/N$ because for $\sigma = 1$, $i_S = 0$ and for $\sigma \ll 1$ the wanted signal $i_{\rm SE} \ll i_{\rm PE}$.

#### *2. Measurement of the emitted electrons with a collector*

With a positive collector with a large solid angle of collection the collector current $i_C = i_{\rm RE} + i_{\rm SE}$ can be measured. With a small solid angle of collection only those RE are measured which can be deflected by the positive potential toward the collector. With a small negative potential at the collector we get $i_C = i_{\rm RE}$.

#### *3. Open multiplier and channeltron*

SE were collected using an electron multipler with Cu-Be dynodes by Smith and Oatley (1955). The use of a channeltron was discussed by Hantsche and Schreiber (1970). Problems are especially the change of the yield with time and the limited lifetime.

#### *4. Everhart–Thornley detector [Fig. 18(a)]*

For SE images in the SEM mostly a scintillator/photomultipler is used (Everhart 1958; Everhart and Thornley 1960). It consists of a scintillator at the end of a light pipe, surrounded by a shielding cage with a metal grid at one end. The scintillator is covered with a very thin layer of aluminum and held at about + 10 kV. The cage is directed towards the specimen and held at some potential: with a potential of + 200 V most of the released SE in the SEM are collected. With a potential of − 100 V only the RE which are emitted in the direction of the collector are measured. The light pipe ends at a vacuum window, pointing to a photomultiplier tube. To collect the SE the specimen is tilted towards the cage and the SE are drawn to the cage and towards the collector. Most of them travel through the grid, are accelerated to the coated scintillator, pass through the aluminum film, and create photons. This light is conveyed by the light pipe to the photomultiplier and converted into electrical signals.

According to Everhart (1958, 1959), 65% of the signal stems from SE, 5% from RE, and 30% from SE released by RE at the walls of the SEM. This detector is suitable for currents in the range of $10^{-6}$–$10^{13}$ A. Light pipe and vacuum feedthrough losses typically reduce the signal to 35% of the created photons.

The noise of different detection systems for SE and RE using a scintillator/photomultiplier combination was studied by Baumann and Reimer (1981). Very interesting are the investigations by Austrata *et al.* (1978, 1982) to use single



Downloaded 28 Jan 2009 to 146.137.148.78. Redistribution subject to AIP license or copyright; see http://jap.aip.org/jap/copyright.jsp

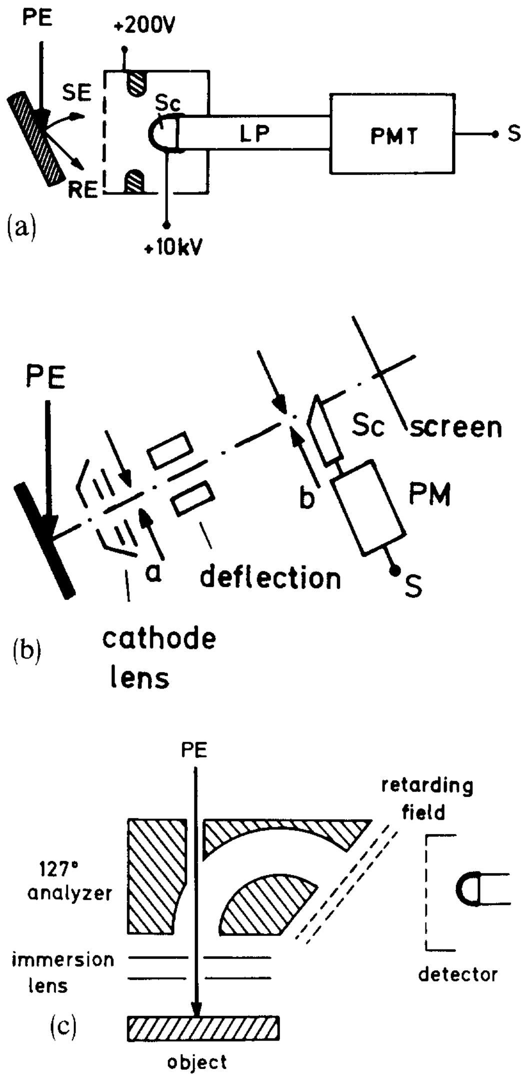


FIG. 18. Detectors for measuring of the emitted electrons in a SEM. (a) Everhart–Thornley detector: combination of a scintillator Sc, a light pipe LP, and a photomultiplier tube PMT. (b) Detector for imaging the surface with SE from a small area around the PE beam according to Hasselbach (1983). a, b Apertures. (c) Detector for quantitative measurement of voltage contrast according to Menzel and Kubalek (1981).

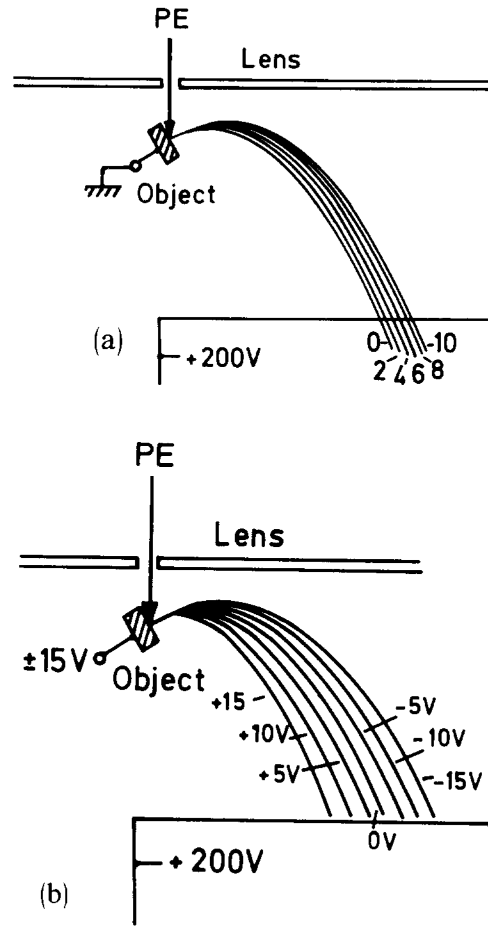


FIG. 19. Deflection of SE emitted normal to the surface with energies from (a) 0–10 eV and (b) by an object at potentials from − 15 to + 15 V in the electric field between final lens and detector at + 200 V according to Everhart (1968).

crystal yttrium aluminum garnet (YAG) activated with cerium as scintillator for SE and PE. The advantage is its high relative efficiency; this involves losses due to optical matching, spectral transmittance of the light pipe, losses on the photocathode of the multiplier, and losses due to insufficient technological optimization of the scintillator.

The SE emitted from the specimen travel different trajectories in the electric field between the lens and the collector according to their different initial energies and momenta. Figure 19(a) shows the trajectories of SE leaving the object surface with energies from 0 to 10 eV towards the collector at + 200 V. Figure 19 (b) shows the deflection of SE starting of an object at different potentials from − 15 to + 15 V (Everhart 1958, 1968). Computation of trajectories in voltage contrast detectors were published by Kursheed and Dinnis (1983).

### *5. Detector for imaging the surface only with SE released from a small sample area [Fig. 18(b)]*

This detector by Hasselbach *et al.* (1983) is similar to the arrangement for measuring the radial spread of the SE (Sec. I I). The cathode lens gives an enlarged image of the specimen in the plane of the fluorescent screen. The aperture "*a*" in the focal plane of the cathode lens prevents the RE from reaching the image plane. The aperture "*b*" selects the circle plane of the object surface contributing to the signal at the scintillator. The deflection element is driven in synchronism with the scanning of the PE beam in order to compensate for the deflection of the PE beam. Only SE released in a small area around the PE beam are focussed on the scintillator, so contrast may be increased.

### *6. Detector for quantitative measurement of voltage contrast [Fig. 18(c)]*

The voltage contrast can be measured in the SEM by passing the SE through an electrostatic energy analyzer between specimen and the electron detector (Wells and Bremer 1968). Another arrangement consists (Menzel and Kubalek 1981) of an immersion or cathode lens for the generation of a high extraction field, a 127° analyzer, a retarding



Downloaded 28 Jan 2009 to 146.137.148.78. Redistribution subject to AIP license or copyright; see http://jap.aip.org/jap/copyright.jsp

field analyzer and an Everhart–Thornley detector. It allows the measuring of small potential differences between adjacent object details (see Voltage II contrast).

### B. SE signal in the SEM

In the conventional SE imaging mode in the SEM several different SE signals reach the detector: see Fig. 2 (Schur *et al.* 1967; Seiler 1968a; Reimer and Pfefferkorn 1977; Peters 1982a,b).

SE (1) signal: SE produced only by PE: $\delta_{\rm PE}$;
SE (2) signal: SE produced by RE at the surface of the specimen: $\eta\delta_{\rm RE}$;
SE (3) signal: SE produced by RE at the walls of the SEM: $\alpha\eta\delta_{\rm Walls}$;
RE (4) signal: RE which reach the detector because they are emitted in this direction.

The SE (1) signal is the desired signal for high resolution, because the SE are emitted at the impact point of the PE beam. This signal is however very sensitive to the conditions of the surface. In a normal SEM we often get a contamination layer at the surface and so the material contrast is poor, compared with topography contrast. In general the SE (2) signal may decrease the lateral resolution because of the lateral spread of the RE. This signal gives however high material contrast because often differences in $\eta$ are greater than in $\delta$. Moreover, this material contrast is nearly independent of thin contamination layers. This signal also makes it possible to see details within the specimen far beyond the escape depth of the SE. This will be discussed in Sec. II H (Information Depth).

The SE (3) signal may increase the SE (2) signal. This is useful to get a high material contrast. Reimer and Volbert (1979) used a negatively biased MgO coated converter plate below the pole piece of the final lens to increase this SE (2) signal.

The SE (3) signal decreases the lateral resolution like the SE (2) signal. In order to decrease the SE (3) signal a RE-absorption plate (a carbon coated aluminum plate with a very low SE yield) can be used (Peters 1982a,b) or a positively biased converter plate below the pole piece of the final lens to prevent SE released by the RE from leaving this plate (Baumann and Reimer 1981). The RE (4) signal depends on the position of the collector relative to the object. It can be prevented using special detectors with a cathode lens (immersion objective) (Hasselbach and Rieke 1982; Menzel and Kubalek 1981). In the cathode lens the slow SE are focussed by an electric field. An aperture in the focal plane of the cathode lens prevents the RE from reaching the collector.

A further SE signal was shown by Hasselbach and Rieke (1976) on objects with sharp edges using a SEM with a special detector with a cathode lens. If the PE beam hits the specimen close to sharp edges, the scattered primaries leaving the edges may again hit the specimen far from their original impact point contributing again to the SE yield (Wells 1978).

The normal SE signal in the SEM is a mixture of different contrast mechanisms. The use of multidetector system makes it possible to isolate one wanted signal. For imaging the specimen surface the SE (1) signal is wanted, the SE (2) signal confuses the detection of surface properties. The SE (2) signal is however proportional to $\eta$. So if we measure the RE signal $\eta$ with another detector we can perform a subtraction: SE signal minus $k\cdot\eta$, so we may be able to select a value of the constant $k$ to enhance surface details by producing a signal which approximately consists only of SE (1) signal (Crewe and Lin 1976; Reimer 1982; Volbert 1982).

### C. Changes of SE emission with time

In the SEM, the SE yield may change with time. In normal vacuum systems a contamination layer can be built by PE and also by RE. The formation of insulating films under electron or ion bombardment was discovered by Stewart (1934). Several papers have been written on this subject and have been summarized by Hren *et al.* (1979) and Love *et al.* (1981). Figure 7 shows the decrease of the SE yield of an Al target depending on the thickness of the contamination layer. With fine electron probes contamination rates of 50 nm/s are possible.

In the SEM the contamination is to be seen as a dark area when the magnification is decreased. On thin foils the contamination may increase the brightness of the field under investigation as shown by Martin (1971).

Changes in SE yields, depending on electron beam dose may also occur under UHV conditions (Le Gressus *et al.* 1979).

The electron beam can produce electron stimulated desorbtion and alter the surface composition of the investigated object. In insulators, as for example in glasses, the electron beam breaks bonds and forms ion-electron pairs and raises the temperature of the material. Both effects cause an increase in alkali ion mobility. During the electron bombardment an electron field within the insulating objects builds up and forms a diffuse negative charge layer at a depth up to the range of the PE. This electric field can cause a field assisted alkali ion diffusion (Ohuchi *et al.* 1980). Specimen charging is a serious problem in the SEM. A summary of charging effects relating to the internal electrical fields and especially to the external fields was given by Shaffner and Hearle (1976).

### D. Contrast in the SEM

Different SE yields of adjacent object elements cause different brightness between the corresponding picture elements (Knoll and Theile 1939; Smith and Oatley 1955; Wells 1957; Everhart *et al.* 1959). The difference in intensity $\Delta I$ of object elements $A$ and $B$ must be greater than the signal/noise ($S/N$). In this part only the contrast of large parts of the specimen will be estimated. The contrast is given by

$$C=\frac{I_A-I_B}{I_A+I_B}=\frac{\Delta I}{2\overline{I}},$$

with

$$\overline{I}=(I_A+I_B)/2. \tag{17}$$

There are different types of contrast in the SEM (Only contrasts due to differences in $\delta$ are considered):



Downloaded 28 Jan 2009 to 146.137.148.78. Redistribution subject to AIP license or copyright; see http://jap.aip.org/jap/copyright.jsp

(1) Material contrast due to different materials at the surface.

(2) Topography contrast due to different inclinations of surface details.

(3) Electron channeling and crystallographic contrast due to different crystallographic orientation with respect to the PE beam.

(4) Voltage type I contrast due to different $\delta$ for different energies of the PE at electrically floating object details.

(5) Voltage type II contrast due to different potentials at surface details often combined with (6).

(6) Voltage type III contrast due to the deflection of SE in the electric fields at the surface.

(7) Voltage contrast at the surface of ferroelectrics.

(8) Magnetic type I contrast due to the deflection of SE in magnetic fields at the surface.

### *1. Material contrast*

*a. Clean surfaces.* This contrast caused by surface materials with different SE yields. The difference in intensity $\Delta I$ is at its maximum for material $A$ with $\delta_A^m$ $(E_A^m)$ and material $B$ with $\delta_B^m$ $(E_B^m)$ when the energy of the PE is either $E_A^m$ or $EE_B^m$. These energies are normally not used in SEM because of the low brightness of the electron guns at low PE energies and the high contamination rates. According to formula (16) the SE yield can be estimated for 20 keV. So

$$C = \frac{(\delta_A^m)^{1.35} - (\delta_B^m)^{1.35}}{(\delta_A^m)^{1.35} + (\delta_B^m)^{1.35}}. \tag{18}$$

For an object consisting of Ti: $\delta^m = 0.8$ and Pt: $\delta^m = 1.35$ we get with SE $E_{\text{PE}} = 20$ keV: $C_1 = 0.34$; and with RE Ti: $\eta = 0.3$, Pt: $\eta = 0.43$ we get $C_2 = 0.18$.

*b. Contaminated surfaces.* In this case we must consider in Eq. (3) if the difference between $\delta_A$ and $\delta_B$ is caused by different $\delta_{\text{PE}}$ or by different $\eta$. In the first case $\eta_A = \eta_B$; $\delta_{\text{PE}}^A \neq \delta_{\text{PE}}^B$ the contrast disappears quickly with increasing thickness of the contamination layer: $C_3 = 0$.

In the second case $\eta_A \neq \eta_B$; $\delta_{\text{PE}}^A \approx \delta_{\text{PE}}^B$ we have a material contrast even with a contamination layer.

$$C_4 = \frac{\beta(\eta_A - \eta_B)}{2 + \beta(\eta_A + \eta_B)}. \tag{19}$$

For Ti: $\eta = 0.3$ and Pt. $\eta = 0.43$ we get with $\beta = 2$: $C_4 = 0.08$. In this case, which we have normally in the SEM, the contrast is less than using RE. However in a UHV-SEM we can get a higher contrast using SE, especially with low energy PE.

### *2. Topography contrast*

The topography contrast is caused by the dependence of $\delta$ on the angle of incidence [Fig. 20(a)] Object details with different inclinations $\vartheta$ and $(\vartheta + \Delta\vartheta)$ with respect to the PE beam are imaged with different brightness. From Eq. (2), $\delta = \delta_0 (\cos\vartheta)^{-n}$ follows for $n = 1$ for the contrast between the planes with the inclination $\Delta\vartheta$

$$C = [\cos\vartheta - \cos(\vartheta + \Delta\vartheta)]/[\cos\vartheta + \cos(\vartheta + \Delta\vartheta)] \tag{20a}$$

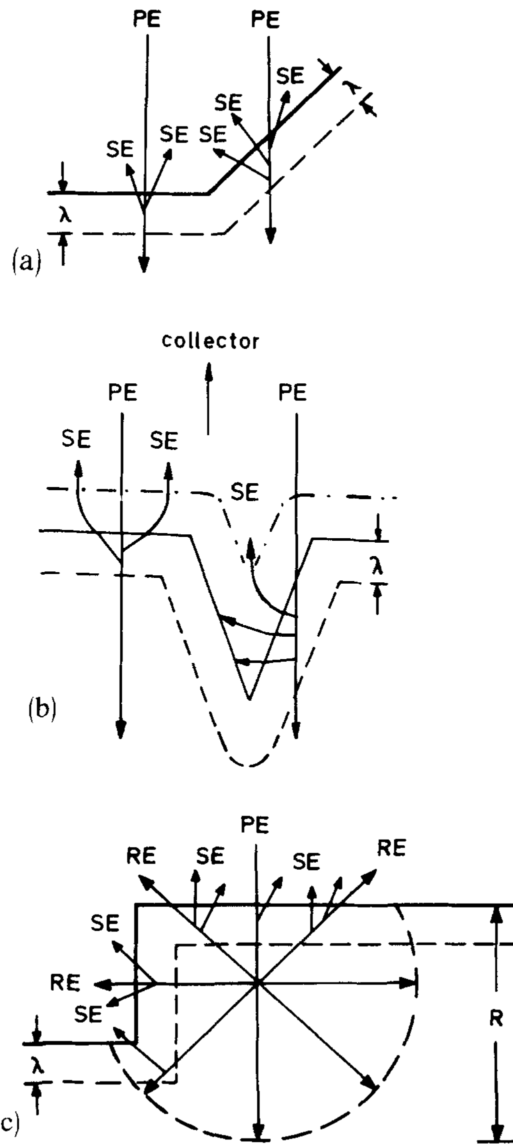


FIG. 20. Topography contrast in the SEM. (a) Different inclinations of object details with respect to the PE beam cause different SE yields. (b) Shadowing effect: the extraction field of the detector is not strong enough to collect all emitted SE. (c) Edge effect: edges within the scattering cloud of the electron beam give a higher SE yield than plane surface parts. $R$: range of the PE.

for $\vartheta = 0$ follows

$$C_1 = (1 - \cos\Delta\vartheta)/(1 + \cos\Delta\vartheta) = \tan^2(\Delta\vartheta/2) \tag{20b}$$

for two planes with a fixed small inclination $\Delta\vartheta$ we get for $\vartheta \neq 0$

$$C_2 = \frac{\Delta\vartheta}{2}\tan\vartheta.$$

So a small topography contrast due to small differences $\Delta\vartheta$ can be enhanced by tilting the object to higher values of $\vartheta$ (Everhart 1958): for $\vartheta = 0°$, $\Delta\vartheta = +10°$ results in $C = 0.007$; for $\vartheta = 50°$, $\Delta\vartheta = +10°$ results in $C = 0.125$. This is valid for a surface with only small angular variations. If the surface is rough, the collection efficiency of the collector must be considered too.

In deep notches the field strength of the electric field



Downloaded 28 Jan 2009 to 146.137.148.78. Redistribution subject to AIP license or copyright; see http://jap.aip.org/jap/copyright.jsp

between specimen and collector is sometimes too small to collect all emitted SE. The electrical field strength at a smooth surface is less than 100 V/cm if a collector potential of 250 V is used. In deep notches the electrical field is smaller and so the image contrast depends on both the energy distribution and the angular distribution of the emitted SE [Fig. 20(b)]. This shadowing effect is however not so strong as with RE.

At edges we get a very high SE yield [Fig. 20(c)]. One contribution is given because the path length of the PE within the escape depth of the SE along the edge is large. More important is the effect that the edge can be within the scattering cloud of the PE and RE. This results in a high SE yield. This part of the edge effect depends on the range of the PE. Fine object structures at the surface are better resolved at low PE energies.

### 3. Voltage contrast

*Voltage type I contrast [Fig. 21(a)].* The SE yield depends on the energy of the PE striking the surface. Different energies of the PE at the surface may not arise only due to different beam energies, but also to different potentials of object details. This can be caused by charging of electrical floating object details. As shown in Sec. I C the second crossover $E^{\rm II}_{\rm PE}$ in the curve $\delta$ depending on $E_{\rm PE}$ (see Fig. 6) represents a stable equilibrium. The different potentials of object details can be produced with an additional electron beam. Image contrast in SEM can be used for a contactless testing of electrical networks as shown by Pfeiffer *et al.* (1981), Brünger (1982), Pfeiffer (1982), and Hohn *et al.* (1982).

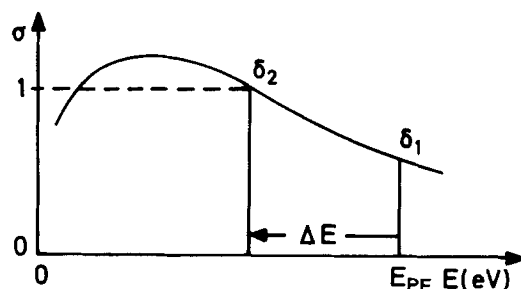


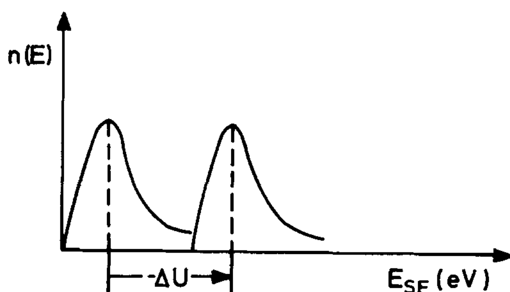


FIG. 21. Voltage contrast in the SEM. (a) Voltage type I contrast: the SE yield $\delta$ depends on the energy of the impinging PE. A negative charging of electrical floating object details causes a deceleration of the PE resulting in a higher yield. (b) Voltage type II contrast: a change of the surface potential ($-\Delta U$) causes a shift of the whole energy distribution of the SE.

*Voltage type II contrast [Fig. 21(b)].* The energy distribution of SE is fixed relative to the potential of the surface. A change of the surface potential causes a shift of the energy spectrum of the SE. Recording the energy distribution of the emitted SE with an energy analyzer gives a possibility to measure the surface potential (Everhart 1958; Wells and Bremer 1968; Menzel and Kubalek 1981). The basis of quantitative voltage measurements is the fact that all electrons of the SE spectrum emitted from an electrode at a certain potential gain the same kinetic energy towards the detector. In this way the whole spectrum is linearly shifted with the applied specimen voltage. The linear shift of the maximum of the spectrum is then a direct measure of the applied specimen voltage. Acccording to Gopinath(1977) the voltage resolution, i.e., the minimum measurable voltage in the SEM, for retarding field analyzers depends on the signal-to-noise ratio, the bandwidth of the detection system, and the primary electron beam current. The detection of voltage differences of about 1 mV is possible (Menzel and Kubalek 1979).

*Voltage type III contrast.* This may be caused by the deflection of the slow SE by electric fields parallel to the surface between different object details. This is similar to the magnetic type I contrast in SEM.

*Voltage type IV contrast.* The domain structure of ferroelectrics gives a contrast in SEM. This may partially be due to voltage III contrast. On the basis of a surface layer, Uchikawa (1982) presented a theory which incorporates the effect of local electrical fields produced across the surface layer by the underlying spontaneous polarized charge onto the SE yield.

### 4. Magnetic type I contrast

A contrast in SEM pictures may arise from the influence of magnetic fields of the specimen. The magnetic fields especially those parallel to the surface can deflect the slow SE so that they cannot reach the detector (Gentsch and Reimer 1972). The magnetic type II contrast shows the influence of internal magnetic fields, deflecting the PE and RE within the specimen.

### 5. Electron channeling and crystallographic contrast

The monotonic increase of $\delta$ with increasing angle of incidence away from the surface normal is only to be seen on amorphous or microcrystalline surfaces. On single crystal targets there are maxima and minima superimposed to the monotonic increase (Fig. 9). This causes the ECP in SEM (Joy *et al.* 1982). ECP can be obtained in the SEM with either SE or RE. The contrast of ECP, registered with SE, depends very sensitively on thin amorphous layers or contamination at the surface. The Bloch waves (Sec. I E) are strongly attenuated with increasing depth, and the ECP are formed in a layer near the surface. So the energy of those RE which give the ECP is near to the energy of the PE and so $\beta$ is smaller than usual (Seiler *et al.* 1970; Seiler 1976). This is in accordance with the high contrast of the ECP in "Low Loss" SEM (Wells 1971).



Downloaded 28 Jan 2009 to 146.137.148.78. Redistribution subject to AIP license or copyright; see http://jap.aip.org/jap/copyright.jsp

## E. Information depth in the SEM using SE

The information depth $D_i$ is defined as the depth below the surface of the object contributing to the SEM picture. Object details in a depth $d$, with $d \leqslant D_i$ can be recognized. $D_i$ depends on the minimal contrast which is detectable in the SEM, on the maximum exit depth of RE, even if SE are used for imaging, and on the difference $\Delta\eta$ in the backscattering coefficients between the object detail and the adjacent material (Seiler 1976; Wells *et al.* 1982). Figure 22 shows an object detail of material $B$ ($\eta_B$) embedded in material $A$ ($\delta,\eta_A$) in a depth $d$.

The intensity in the object detail $A$ is

$$I_A = I_{\rm PE}\,\delta_{\rm PE} + I_{\rm PE}\,\eta_A\,\delta_{\rm RE}. \tag{21}$$

The intensity at the surface of the specimen above object detail $B$ is the sum of

$I_{B1} = I_{\rm PE}\,\delta_{\rm PE}$,

$I_{B2}$ = those SE, released by the RE backscattered in material $A$,

$I_{B3}$ = those SE, released by the RE backscattered in material $B$. With increasing thickness $d$ of the layer the intensity of the PE decreases.

For a rough estimate of the information depth we assume that the number of penetrating electrons in a layer of the thickness $d$ decreases with $I_{\rm PE}e^{-4d/R}$ with $R$ the range of the PE. The maximum of the escape depth of the RE is about $R/2$ and the number of the RE according to their lower mean energy decreases in a layer of a thickness $d$ with $I_{\rm RE}$ $e^{-8d/R}$ (Seiler 1976). The difference $\Delta I$ in intensities of the SE is

$$I = I_{\rm PE}\delta_{\rm RE}(\eta_A - \eta_B)\,e^{-8d/R}. \tag{22}$$

The contrast in the SEM for SE with $\beta = 2$ and the mean value $\bar\eta = 0.25$ is

$$C = \frac{\Delta I}{2I_{\rm PE}(\delta_{\rm PE} + \bar\eta\delta_{\rm RE})} \approx 0.67\,(\eta_A - \eta_B)e^{-8d/R} \tag{23}$$

and with Eq. (12) we get the information depth

$$D_i = R/8\,\ln[67(\eta_A - \eta_B)], \tag{24}$$

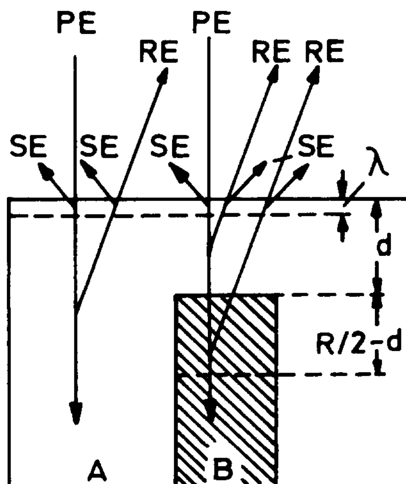


FIG. 22. Test object for measuring the information depth in the SEM. $R$: range of the PE.

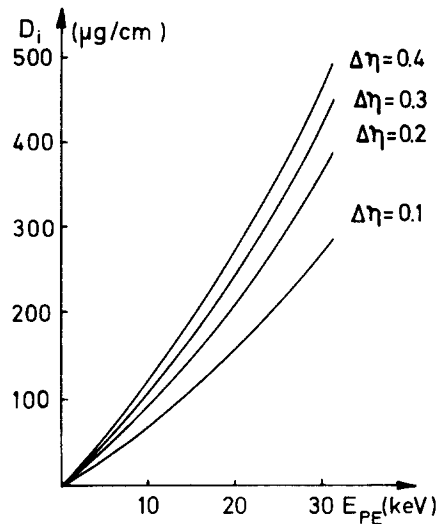


FIG. 23. Information depth in the SEM as a function of $E_{\rm PE}$.

and with Eq. (12) we get the information depth

$$\frac{D_i}{\mu{\rm g/cm}^2} = 1.4\,\ln[(67\,\Delta\eta)]\left(\frac{E_{\rm PE}}{\rm keV}\right)^{1.35}. \tag{25}$$

Figure 23 shows these functions for various $\Delta\eta$ which agree rather well with experimental results. Figure 24 shows an example for the dependence of the information depth on the energy on the PE. The estimate of the information depth is similar to the measuring of the thickness of layers of RE (Hohn *et al.* 1976; Wells *et al.* 1982). Calculations on the dependence of SEM contrast upon electron penetration were published by George and Robinson (1976).

## F. Lateral resolution in the SEM using SE

(a) Signal/Noise ratio. In order to discriminate between adjacent picture elements by their different brightness, the difference in the signal quanta caused by the released SE must be high enough compared with the statistical fluctuations. A beam of $10^{-11}$ A is satisfactory for most objects (Oatley 1981; Broers 1982).

(b) The diameter of the PE beam. The beam diameter in which we can focus a beam depends on the primary beam energy, the brightness of the electron gun, the energy spread of the electron beam, the chromatic aberration coefficient of the final lens $C_c$, the spherical aberration coefficient of the final lens $C_s$, and the focal length of the final lens (Nagantani and Ohura 1977).

Figure 25 shows the minimal beam diameter for a beam with $10^{-11}$ A at 25 keV with $C_s = 18$ mm, $C_c = 11$ mm depending on the brightness of the electron gun with an energy spread of 0.3 eV typical of a field emission gun. Using thermal cathodes the energy spread is normally greater (Broers 1982).

(c) The spatial emission distribution of SE. The spatial emission distribution of the SE (1) signal is much smaller than the spatial emission distribution of the SE (2) signal and of the RE. If the SE (1) signal is strong enough compared with SE (2) signal the resolution of a SEM using SE is deter-



Downloaded 28 Jan 2009 to 146.137.148.78. Redistribution subject to AIP license or copyright; see http://jap.aip.org/jap/copyright.jsp

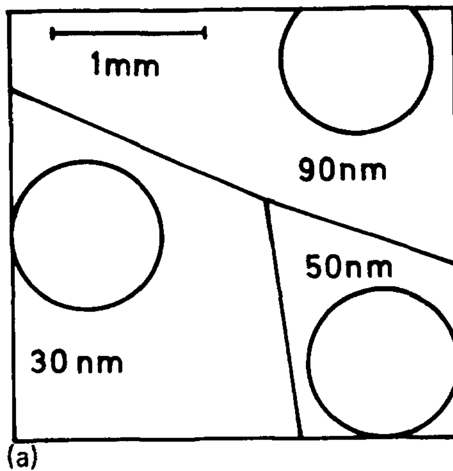


(a)

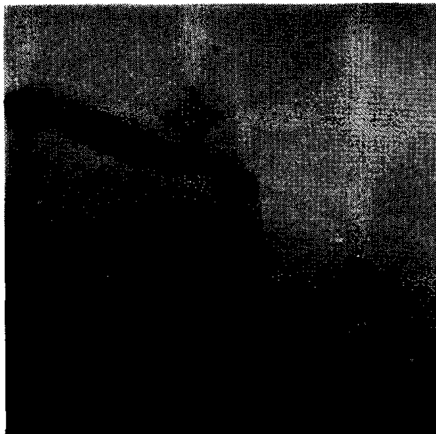

(b)

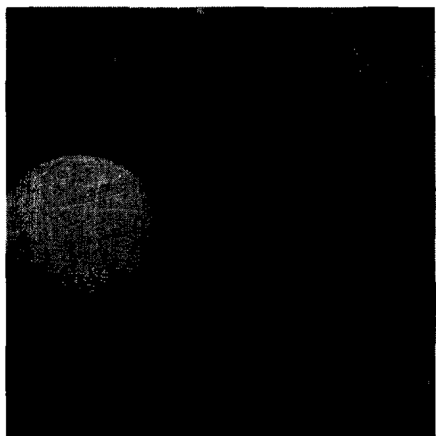

(c)

FIG. 24. Demonstration of the information depth in the SEM depending on the energy of the PE: Gold wires in aluminum under aluminum layers of different thickness. (a) Schematical. (b) $E_{PE} = 1$ keV. (c) $E_{PE} = 3.3$ keV.

mined by the diameter of the PE beam enlarged by the mean-free-path length of the SE in material which is similar to the mean escape depth $\lambda$ of the SE, $\lambda \approx 1$ nm in metals. Because thin metal coatings are used to prevent many insulating samples from charging these results relate to the ultimate resolution that one can expect in a SEM using SE (Everhart and Chung 1972).

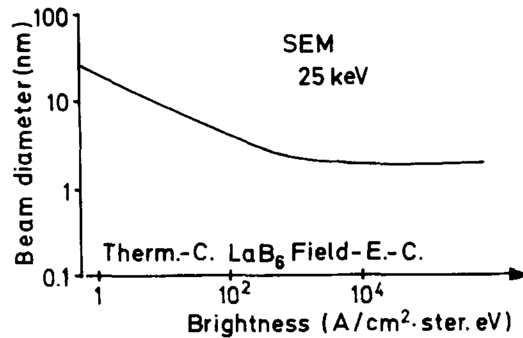


FIG. 25. Minimal beam diameter for a beam current of $10^{-11}$ A depending on the normalized beam brightness for a SEM with $C_s = 18$ mm, $C_c = 11$ mm at 25 keV according to Broers (1982).

## G. Conditions for high resolution in the SEM

To get a beam diameter of about 1 nm with a beam current of $10^{-11}$ A we need a field emission gun. High resolution images are possible with the SE (1) signal (Peters 1982a,b). The SE (3) signal can be suppressed by using an electron absorption device attached to the pole piece of the final lens or a positive converter plate. The main problem is the reduction of the SE (2) signal which has the spatial emission distribution of the RE which decreases the resolution. The use of a multi detector system works at the cost of the $S/N$. Especially for imaging of biological objects with low atomic number the SE (2) signal is weak if the coating metal film to prevent charging is as thin as possible and homogeneous (Evans and Ranks 1981). According to Peters (1982a,b) it is possible to get fine crystalline homogeneous films with a thickness of about 2 nm with the metals tantalum, niobium, and chromium. For these objects the quality of the images in the SE (1) image mode with a SEM with a field emission gun equals according to Peters (1982a) that of images obtained in the transmission electron microscope for identically coated specimens.

## ACKNOWLEDGMENTS

The author thanks Dipl. Phys. H. E. Bauer and Dr. O. C. Wells for many helpful discussions, Professor Dr. T. E. Everhart for valuable hints, Mrs. Jacobi for very careful drawing of the figures, and Mrs. Paukert for patient typing assistance.

## LIST OF ABBREVIATIONS

SE: Secondary electron
SEM: Scanning electron microscope
PE: Primary electron
SEE: SE emission
$\lambda$: Mean escape depth of SE
$T$: Maximum escape depth of SE
UHV: Ultrahigh vacuum
RE: Backscattered or reflected electrons
$E^m_{SE}$: Most probable energy of the SE
HW: Full width at half maximum
$\delta$: SE yield
$\eta$: RE coefficient



Downloaded 28 Jan 2009 to 146.137.148.78. Redistribution subject to AIP license or copyright; see http://jap.aip.org/jap/copyright.jsp

$\sigma$: Total yield: $\sigma = \delta + \eta$
$\eta_E$: Coefficient of elastically reflected electrons
$\delta^m$: SE yield at its maximum
$\delta_{PE}$: SE yield per PE
$\delta_{RE}$: SE yield per RE
$\beta$: $\delta_{RE}/\delta_{PE}$
$E_{PE}$: Energy of the PE
$E_{PE}^m$: Energy of the PE for which $\delta = \delta^m$
$E_{PE}^{I}$: Value of $E_{PE} < E_{PE}^m$ for which $\sigma = 1$
$E_{PE}^{II}$: Value of $E_{PE} > E_{PE}^m$ for which $\sigma = 1$
ECP: Electron channeling pattern
$Z$: Atomic number
$I$: Ionization energy
EEM: Electron emission microscope
$t$: Number of transmitted electrons/number of PE
$\delta_T$: SE yield per transmitted electrons
$\beta_t$: $\delta_T/\delta_{PE}$
$R$: Range of PE
$D_i$: Information depth in the SEM
$\Phi$: Work function
$C$: Contrast


Alig, R. C. and Bloom, S. (1978). "Secondary-electron-escape probabilities," J. Appl. Phys. **49**, 3476–3480.

Appelt, G. (1968). "Fine structure measurements in the energy angular distribution of secondary electrons from a (110) face of copper," Phys. Status Solidi **27**, 657–669.

Ardenne, M. von. (1940). *Elektronen-Übermikroskopie* (Springer, Berlin).

Ardenne, M. von. (1956). *Tabellen der Elektronenphysik, Ionenphysik und Übermikroskopie* (VEB Deutscher Verlag der Wissenschaften, Berlin).

Autrata, R., Schauer, P., and Kvapil, J. (1978). "A single crystal of YAG—New fast scintillator in SEM," J. Phys. E **11**, 707–708.

Autrata, R., Schauer, P., Kvapil, Jo., and Kvapil, Ji. (1982). "A single crystal of $Y_3Al_5O_{12}$:$CE^{3+}$ as a scintillator in SEM and a transparent screen in electron optical devices," Electron Microsc. 1982, 451–452.

Baumann, W. and Reimer, L. (1981). "Comparison of the noise of different electron detection systems using a scintillator-photomutiplier combination," Scanning **4**, 141–151.

Begrambekov, L. V., Kurnaev, V. A. Sotnikov, V. M. and Tel'kovskii, V. G. (1971), "Anisotropy in the angular distribution of ion-electron emission from a niobium single crystal," Sov. Phys.-Solid State **13**, 379–380.

Beisswenger, S. and Gruner, H. (1974). "The secondary electron emission frin Be-BeO transition layers reactively deposited by evaporation," Optik **40**, 518–538.

Bouchard, C. and Carette, J. D. (1980). "The surface potential barrier in secondary emission from semiconductors," Surf. Sci. **100**, 241–250.

Broers, A. N. (1982). "Resolution in surface scanning electron microscopy of bulk samples." Ultramicroscopy **8**, 137–144.

Bronshtein, I. M. and Denisov, S. S. (1967). "Secondary electron emission of Aluminum and nickel obliquely incident primary electrons," Sov. Phys.-Solid State **9**, 731–732.

Bronshtein, I. M. and Dolinin, V. A. (1968). "The secondary electron emission (SEE) of solids at large angles of incidence of primary beam," Sov. Phys.-Solid State **9**, 2133–2140.

Bronshtein, I. M. and Fraiman, B. S. (1969). *Secondary Electron Emission* (Nauka, Moscow).

Bruenger, W. H., Hohn, F. J., Kern, D. P., Coane, P. J., and Chang, T. H. P. (1982). "Electron energy analyzer for applications in large scan field electron beam testing," 10th International Conference on Electron and Ion Beam Science and Technology (1982) (in press).

Bruining, H. (1954). *Physics and Application of Secondary Electron Emission* (Pergamon, London).

Buchholz, J. (1969). "On the position of the maximum of the secondary electron yield curve," Z. Phys. **227**, 440–452.

Burns, J. (1960). "Angular distribution of secondary electrons from (100)-faces of Cu and Ni," Phys. Rev. **119**, 102–14.

Cailler, M., Ganachaud, J. P., and Roptin, D. (1981). "Pénétration d'un faisceau d'électrons dans une cible métallique et emission électronique induite," Le Vide (Couches Minces) **36**, 279–294.

Cailler, M., Ganachaud, J. P., and Bourdin, J. P. (1981). "The mean free path of an electron path of an electron in copper between two inelastic collisions," Thin Solids Films **75**, 181–189.

Carle, W. and Seiler, H. (1966). "Beobachtungen des Bildkkontrastes im Elektronen-Emissionsmikroskop," Optik **24**, 305–312.

Chase, R. E. Gordon, W. L., and Hoffmann, R. W. (1980). "Measurement of low energy secondary electron distribution using a double-pass cylindrical mirror analyzer," Appl. Surf. Sci. **4**, 271–281.

Chung, M. S. and Everhart, T. E. (1974). "Simple calculation of energy distribution of low-energy secondary electrons emitted from metals under electron bombardment," J. Appl. Phys. **45**, 707–709.

Chung, M. S. and Everhart, T. E. (1977). "Role of plasmon decay in secondary electron emission in the nearly free electron metals-application to aluminum," Phys. Rev. B **15**, 4699–4715.

Copeland, P. L. (1940). "Secondary emission from films of platinum on aluminum," Phys. Rev. **58**, 604.

Crewe, A. V. and Lin, P. S. D. (1976). "The use of backscattered electrons for imaging purposes in a scanning electrons microscope," Ultramiscroscopy **1**, 231–238.

Dekker, A. J. (1958). "Secondary electron emission," Solid State Phys. **6**, 251–315.

Dietrich, W. and Seiler, H. (1960). "Energieverteilung von Elektronen, die durch Ionen und Elektronen in Durchstrahlung dünner Folien ausgelöst werden," Z. Phys. **157**, 576–585.

Drescher, H., Reimer, L., and Seidel, H. (1970). "Rückstreukoeffizient und Sekundärelektronen-Ausbeute von 10–100 keV-Elektronen und Beziehungen zur Raster-Elektronenmikroskopie," Z. Angew. Phys. **29**, 331–336.

Evans, A. C. and Franks, J. (1981). "Specimen coating for high resolution scanning electron microscopy," Scanning **4**, 169–174.

Everhart, T. E. (1958). "Contrast formation in the SEM," Ph.D. dissertation Cambridge University.

Everhart, T. E., Wells, O. C., and Oatley, C. W. (1959). "Factors affecting contrast and resolution in the scanning electron microscope," J. Electron. Control. 7, 97–111.

Everhart, T. E. and Thornley, R. F. M. (1960). "Wide-band detector micro-microampere low-energy electron curents," J. Sci. Instrum. **37**, 246–248.

Everhart, T. E. (1968). "Reflections and scanning electron microscopy," Scanning Electron Microsc. 1968, 1–12.

Everhart, T. E. (1970). "Contrast and Resolution in the SEM," Third Stereoscan SEM Colloquium, Kent Cambridge Sci. Inc., 1–8.

Everhart, T. E. and Chung, M. S. (1972). "Idealized spatial emission distribution of secondary electrons," J. Appl. Phys. **43**, 3708–3711.

Filippov, Yu. A. (1966). "Statistics of secondary electron emission for nickel and iron,"' Sov. Phys.-Solid State **8**, 701–705.

Fitting, H. J. (1974). "Transmission, energy distribution and secondary electron excitation of fast electrons in thin solid films," Phys. Status Solidi A **26**, 525–535.

Fitting, H. J., Glaefeke, H., Wild, W., and Neumann, G. (1976). "Multiple scattering of fast electrons and their secondary electron generation within semi-infinite targets," J. Phys. D **9**, 2499–2510.

Fitting, H. J. (1980)."Some aspects of electron emission from solids," Exp. Tech. Phys. **28**, 321–329.

Ganachaud, J. P. and Cailler, M. (1979). "A Monte Carlo calculation of the secondary electron emission of normal metals," Surf. Sci. **83**, 498–530.

Gentsch, P. and Reimer, L. (1972). "Messungen zum magnetischen Kontrast im Raster-Elektronenmikroskop," Beiträge Elektr. Direktabb. Oberflächen (BEDO) (edited by G. Pfefferkorn) **5**, 299–312.

George, E. P. and Robinson, V. N. E. (1976). "The dependence of SEM contrast upon electron penetration," Proc. SEM Conf. (1976) (edited by O. Johari) **I**, 18–23.

Goetze, G. W., Boerio, A. H., and Green, M. (1964). "Field enhanced secondary electron emission from films of low density," J. Appl. Phys. **35**, 482–489.

Goetze, G. W. (1968). "Secondary electron conduction (SEC) and its application to photo-electronic image devices," Adv. Electron. Electron Phys. **22**, 219–227.

Goldstein, J. I. and Yakowitz, H. (1975). *Practical Scanning Electron Microscopy* (Plenum, New York).




Downloaded 28 Jan 2009 to 146.137.148.78. Redistribution subject to AIP license or copyright; see http://jap.aip.org/jap/copyright.jsp

Gopinath, A. (1977). "Estimate of minimum measurable voltage in the SEM," J. Phys. E. **10**, 911–913.

LeGressus, C., Massignon, D., Mogami, A., and Okuzumi, H. (1979). "Secondary electron emission dependence on electron beam density dose and surface interactions from AES and ELS in an ultra high vacuum SEM," Proc. SEM Conf. (1979), edited by O. Johari, pp. 161–172.

Grunder, M. and Halbritter, J. (1980). "On surface coatings and secondary yield of $Nb_3Sn$ and Nb," J. Appl. Phys. **51**, 5396–5405.

Halbritter, J. (1982). "On conditioning: Reduction of secondary- and rf-field emission by electron, photon, or helium impact," J. Appl. Phys. **53**, 6475–6478.

Halbritter, J. (1983). "Resonant emission of SE," Proc. SEM Conf. (1983) edited by O. Johari (in press).

Hachenberg, O. and Bauer, W. (1959). "Secondary electron emission from solids," Adv. Electron Electron Phys. **11**, 413–499.

Hantsche, H. and Schreiber, G. (1970). "Zur Verwendung eines Channeltrons als Elektronendetektor im Raster-Elektronenmikroskop," Beiträge Elektr. Direktabb. Oberflächen (BEDO) (edited by G. Pfefferkorn) **3**, 167–178.

Hasselbach, F. (1973). "Messung der Ortsverteilung von gestreuten Elektronen in Durchstrahlung und Reflexion im Elektronenemissionionsmikroskop," Thesis Tübingen.

Hasselbach, F. (1975). "Emissionsmikroskopische Messung der Ortsverteilung von 20 keV Elektronen nach Streuung in dunnen Al- und Ge Aufdampfschichten," Z. Phys. **22**, 151–159.

Hasselbach, F. and Rieke, U. (1976). "Emission microscopical investigation of the edge brightening effect in the SEM," 6th European Congress on Electron microscopy, Jersalem, pp. 296–298.

Hasselbach, F. and Rieke, U. (1978). "Emission microscopical investigation of the proximity effect in electron beam lithography," *9th International Congress on Electron Microscopy, Toronto*, edited by J. M. Sturgess (Imperial, Canada), Vol. 1, pp. 166–167.

Hasselbach, F. and Rieke, U. (1982). "Spatial distribution of secondaries released by backscattered electrons in silicon and gold for 20–70 keV primary energy," 10th International Congress on Electron Microscopy, Hamburg, edited by the Congressional Organization Committee, Deutsche Ges. EM, Vol. 1, pp. 253–254.

Hasselbach, F., Rieke, U. and Straub, M. (1983). "An imaging secondary electron detector for the SEM," Proc. SEM Conf. (1983), edited by O. Johari (in press).

Hohn, F. J. Kindt, M., Niedrig, H. and Stuth, B. (1976). "Elektronenrückstreumessungen an dünnen Schichten auf massiven Trägersubstanzen," Optik **46**, 491–500.

Hohn, F. J., Chang, T. H. P., Kern, D., Bruenger, W., Coane, P., and Lindemann, M. (1982). "Electron beam testing and its application to package modules for VLSI arrays," SPIE Conf. 1982 (in press).

Holt, D. B. Muir, M. D., Grant, P. R. and Boswarva, I. M. (1974). *Quantitative Scanning Electron Microscopy* (Academic, New York).

Howie, A. (1974). "Theory of diffraction contrast effects in the SEM," in *Quantitative SEM*, edited by D. B. Holt and H. D. Muir, pp. 184–209. pp. 184–209.)

Hren, J. J., Goldstein, J. I., and Joy, D. C. (1979). "Barriers to AEM: Contamination and Etching," in An Introduction to Analytical Electron Microscopy (Plenum, New York), pp. 481–505.

Jahrreiss, H. (1965). "Über einige Erweiterungsmöglichkeiten der Sternglass'schen Theorie der Sekundärelektronen Emission," Ann. Phys. (VII) **14**, 325–352.

Jahrreiss, H. (1972). "Secondary electron emission from thin films," Thin Solid Films **12**, 187–200.

Jonker, J. L. H. (1957). "Secondary electron emission of solids," Phillips Res. Rep. **12**, 249–300.

Joy, D. C., Newbury, D. E., and Davidson, D. L. (1982). "Electron channeling patterns in the scanning electron microscope," J. Appl. Phys. **53**, R81–R122.

Kadlec, J. and Eckertová, L. (1970). "Zur Bestimmung der Sekundärelekronenemission dünner Schichten," Z. Angew. Phys, **30**, 141–145.

Kanaya, K. and Kawakatsu, H. (1972). "Secondary electron emission due to primary and backscattered electrons," J. Phys. D **5**, 1727–1742.

Kanaya, K. and Ono, S. (1978). "The energy dependence of a diffusion model for an electron probe into solid targets, J. Phys. D **11**, 1495–1508.

Kanaya, K., Ono, S., and Ishigaki, F. (1978). "Secondary electron emission from insulators," J. Phys. D **11**, 2425–2437.

Kanter, H. (1961). "Contribution of backscattered electrons to secondary electron formation," Phys. Rev. **121**, 681–684.

Kanter, H. (1970). "Slow-electron mean free paths in aluminum, silver and gold," Phys. Rev. B **1**, 522–536.

Knoll, M. (1935). "Aufladepotential und Sekundäremission elektronenbestrahlter Körper," Z. Tech. Phys. **16**, 467.

Knoll, M. and Theile, R. (1939). "Elektronenabtaster zur Strukturabbildung von Oberflächen," Z. Phys. **113**, 260.

Knoll, M. (1941). "Streuwirkung eines geladenen Teilchens im Feld einer Sekundäremissionskathode," Naturwiss. **29**, 335–336.

Kollath, R. (1956). "Sekundärelektronen-Emission fester Körper bei Bestrahlung mit Elektronen," *Handbuch der Physik* (Springer, Berlin), Vol. 21, pp. 232–303.

Kuhnle, G., Martin, J. P., and Seiler, H. (1969). "Schichtdickenuntersuchung im SEM," Beiträge Elektr. Direktabb. Oberflächen (BEDO) (edited by G. Pfefferkorn) **2**, 101–105.

Kuhnle, G., and Seiler, H. (1974). "Optimale Energie zur Erzeugung der ECP im SEM mit reflektierten Elektronen," Beiträge Elektr. Direktab. Oberflächen (BEDO) (edited by G. Pfefferkorn)

Kurrelmeyer, B. and Hayner, L. J. (1937). "Shot effect of secondary electrons from nickel and beryllium," Phys. Rev. **52**, 952–958.

Kursheed, A. and Dinnis, A. R. (1983). "Computation of trajectories voltage contrast detectors," Scanning **5**, 25–31.

Leamy, H. J. (1982). "Charge collection scanning electron microscopy," J. Appl. Phys. **53**, R51–R80.

Love, G., Scott, V. D., Dennis, N. M. T., and Laurenson, L. (1981). "Sources of contamination in electron optical equipment," Scanning **4**, 32–39.

Makarov, V. V. and Petrov, N. N. (1981). "Regularities of secondary electron emission of elements of the periodic table," Sov. Phys Solid State **23**, 1028–1032.

Malter, L. (1936). "Thin film field emission," **50**, 48–52.

Martin, J. P. (1971), "Zum Einfluss der Objektkontamination auf das rastermikroskopische Bild," Beiträge Elektr. Direktabb. Oberflächen (BEDO) (edited by G. Pfefferkorn) **412**, 387–397.

Mayer, H., and Hölzl, J. (1966). "Experimentelle Bestimmung der maximalen Austrittstiefen monoenergetischer Sekundärelektronen," Phys. Status Solidi **18**, 779–785.

Menzel, E. and Kubalek, E. (1979). "Electron beam test system for VLSI circuit inspection," Proc. SEM Conf. (1979), edited by O. Johari, Vol. 1, pp. 297–304.

Menzel, E. and Kubalek, E. (1981). "Electron beam test techniques for integrated circuits," Proc. SEM Conf. (1981), edited by O. Johari, Vol. 1, pp. 305–322.

Möllenstedt, G. and Lenz, F. (1963). "Electron emission microscopy," Adv. Electron. Electron Phys. **18**, 251–326.

Moncrieff, D. A. and Barker, P. R. (1978). "Secondary electron emission in the scanning electron microscope," Scanning **1**, 195–197.

Murata, K. (1973). " Monte-Carlo calculations on electron scattering and secondary electron production in the SEM," Proc. SEM Conf. (1973), edited by O. Johari, Vol. 2, pp. 267–276.

Nagantani, T. and Okura, A. (1977). "Enhanced secondary electron detection at small working distance in the filed emission SEM," Proc. SEM Conf. (1977), edited by O. Johari, Vol. 1, pp. 695–702.

Niedrig, H. and Sieber, P. (1971), "Rückstreuung mittelschneller Elektronen an dünnen Schichten," Z. Angew. Phys. **31**, pp. 27–31.

Niedrig, H. (1982). "Electron backscattering from thin films," J. Appl. Phys. **53**, R15–R49.

Oatley, C. W. and Everhart, T. E. (1957). "The examination of *p-n* junctions with the SEM," J. Electron. **2**, 578–570.

Oatley, C. W. (1972). *The Scanning Electron Microscope, Part I: The instrument* (Cambridge University, Cambridge).

Oatley, C. W. (1981). "Detectors for the scanning electron microscope," J. Phys. E. **14**, 971–976.

Oatley, C. W. (1982). "The early history of the SEM," J. Appl. Phys. Rev. **53**, R1–R13.

Ohuchi, F., Ogino, M., Holloway, P. H., and Pantano, Jr., C. G. (1980). "Electron beam effects during analysis of glass thin films with Auger electron spectroscopy," Surf. Interface Anal. **2**, 85–90.

Ono, S. and Kanaya, K. (1979). "The energy dependence of secondary emission based on the range-energy retardation power formula," J. Phys. D **12**, 619–632.

Palmberg, P. W. (1967). "Secondary emission studies on Ge and Na-covered Ge," J. Appl. Phys. **38**, 2137–2147.

Peters, K. R. (1980). "Penning sputtering of ultra thin metal films for high resolution electron microscopy," Proc. SEM Conf. (1980), edited by O.



Downloaded 28 Jan 2009 to 146.137.148.78. Redistribution subject to AIP license or copyright; see http://jap.aip.org/jap/copyright.jsp

Johari (1980), Vol. I, pp. 143–154.
Peters, K. R. (1982a). "Conditions for high quality high magnification images in the SE (1) SEM," Proc. SEM Conf. (1982), edited by O. Johari (in press).
Peters, K. R. (1982b). "Generation, collection and properties of an SE (1) enriched signal suitable for high resolution SEM on bulk specimens," Proceedings of the Asilomar Conference 1982 (in press).
Pfeiffer, H. C., Langner, G. O., Stickel, W., and Simpson, R. A. (1981). "Contactless electrical testing of large area specimens electron beams," J. Vac. Sci. Technol. **19**, 1014–1018.
Pfeiffer, H. C. (1982). "Contactless electrical testing with multiple electron beams," Proc. SEM Conf. (1982), edited by O. Johari (in press).
Pillon, J., Roptin, D., and Cailler, M. (1976). "Secondary electron emission from aluminum," Surf. Sci. **59**, 741–748.
Reimer, L., Seidel, H., and Gilde, M. (1968). "Einfluss der Elektronen-diffusion auf die Bildentstehung im SEM," Beiträge Elektr. Direktabb. Oberflächen (BEDO), edited by G. Pfefferkorn, Vol. 1, pp. 53–65.
Reimer, L. (1971). "Rauschen der Sekundarelektronenemission," Beitrage Elektr. Direktabb. Oberflächen (BEDO) (edited by G. Pfefferkorn) **412** 299–304.
Reimer, L. and Drescher, H. (1977). "Secondary electron emission of 10–100 keV electrons from transparent films of Al and Au," J. Phys. D **10**, 805–815.
Reimer, L. and Pfefferkorn, G. (1977). "Rasterelektronenmikroskopie," (Springer, Berlin), pp. 34–59.
Reimer, L. and Drescher, H. (1977). "Secondary electron emission of 10–100 keV electrons from transparent films of Al and Au," J. Phys. D **10**, 805–815.
Reimer, L. and Volbert, B. (1979). "Detector system for backscattered electrons by conversion to secondary electrons," Scanning **2**, 238–248.
Reimer, L. and Tollkamp, C. (1980). "Measuring the backscattering coefficient and secondary electron yield inside a scanning electron microscope," Scanning **3**, 35–39.
Reimer, L. (1982). "Electron signal and detector strategy," Proceedings of the Asilomar Conference 1982 (in press).
Robinson, V. N. E. (1974). "The origins of the secondary electron signal in scanning electron microscopy," J. Phys. D **7**, 2169–2173.
Robinson, V. N. E. (1975). "The dependence of emitted secondary electrons upon the direction of travel of the exciting electron," J. Phys. D **8**, L74–L76.
Rösler, M. and Brauer, W. (1981). "Theory of secondary electron emission," Phys. Status Solidi B **104**, 161–175, 575–587.
Salehi, M. and Flinn, E. A. (1981). "Dependence of secondary-electron emission from amorphous materials on primary angle of incidence," J. Appl. Phys. **52**, 994–996.
Salow, H. (1940). "Sekundärelektronen-Emission," Phys. Z. **41**, 434–442.
Schäfer, J. and Hölzl, J. (1972). "A contribution to the dependence of secondary electron emission from the work function and Fermi energy," Thin Solid Films **18**, 81–86.
Schmid, R., Gaukler, K. H., and Seiler, H. (1983). "Measurement of elastically reflected electrons ($E \leqslant 2.5$ keV) for imaging of surfaces in a simple UHV-SEM," Proc. SEM Conf. (1983), edited by O. Johari (in press).
Schur, K., Schulte, Chr., and Reimer, L. (1976). "Auflösungsvermogen und Kontrast von Oberflächenstufen bei der Abbildung mit einem Raster-Elektronenmikroskop," Z. Angew. Phys. **23**, 405–412.
Seah, M. P. (1969). "Slow electron scattering from metals," Surf. Sci. **17**, 132–213.
Seiler, H. and Stärk, M. (1965a). "Hohe Sekundärelektronen-Emission aus $BaF_2$-Schichten geringerer Dichts," Z. Angew. Phys. **19**, 90–93.
Seiler, H. and Stärk, M. (1965b). "Bestimmung der mittleren Laufwege von Sekundarelektronen in einer Polymerisatschicht," Z. Phys. **183**, 527–531.
Seiler, H. (1967). "Some problems of secondary electron emission," Z. Angew Phys. **22**, 249–263.
Seiler, H. (1968a). "Die physikalischen Aspekte der Sekundärelektronenemission für die Elektronen-Raster-Mikroskopie," Beiträge Elektr. Direktabb. Oberflächen (BEDO) (edited by G. Pfefferkorn) 1, 27–52.
Seiler, H. (1968b). "Abbildung von Oberflächen mit Elektronen, Ionen und Röntgenstrahlen," Bibliographisches Institut, Mannheim.
Seiler, H., Kuhnl, G., and Martin, J. P. (1970). "Die Abhängigkeit der orientierungsabhängigen Reflexe von dem kristallinen Zustand der Oberflache," Beiträge Elektr. Direktabb. Oberflächen (BEDO) (edited by G. Pfefferkorn) **3**, 137–142.
Seiler, H. and Kuhnle, G. (1970). "Anisotropy of the secondary electron yield as a function of the energy of the primary electrons from 5 to 50 keV," Z. Angew Phys. **29**, 254–260.
Seiler, H. (1976). "Determination of the information depth in the SEM," Proc. SEM Conf. (1976) (edited by O. Johari) Vol. **I**, 9–16.
Seiler, H. (1982). "Secondary electron emission," Proceedings of the Asilomar Conference 1982 (in press).
Shaffner, T. J. and Hearle, J. W. S. (1976). "Recent advances in understanding specimen charging," Proc. SEM Conf. (1976) (edited by O. Johari) **1**, 61–70.
Shimizu, R. and Murata, K. (1971). "Monte-Carlo calculations of the electron-sample interactions in the scanning electron microscope," J. Appl. Phys. **42**, 387–394.
Shimizu, R. (1974). "Secondary electron yield with primary electron beam of kilo-electron-volts," J. Appl. Phys. **45**, 2107–2111.
Simon, R. E. and Williams, B. F. (1968). "Secondary electron emission," J. IEEE Trans. Nucl. Sci. **NS-15**, 167.
Smith, K. C. A. and Oatley, C. W. (1955). "The SEM and its fields of application," Brit. J. Appl. Phys. **6**, 391–399.
Sternglass, E. J. and Wachtel, M. M. (1955). "Measurement of low-energy electron absorption in metals and insulators," Phys. Rev. **99A**, 646–650.
Stewart, R. L. (1934). "Insulating films formed under electron and ion bombardment," Phys. Rev. **45**, 488–490.
Thornton, P. R. (1968). *Scanning Electron Microscopy, Applications to Materials and Device Science* (Chapman and Hall, London).
Uchikawa, Y. and Ikeda, S. (1981). "Application of scanning electron microscopy (SEM) to analysis of surface domain structure of ferroelectrics," Proc. SEM Conf. (1981) (edited by O. Johari) **1**, 209–220.
Volbert, B. (1982). "Signal mixing technqiues in SEM," Proceedings of the Asilomar Conference 1982 (in press).
Voreades, D. (1975). "Secondary electron emission from thin carbon films," Surf. Sci. **60**, 325–348.
Wells, O. C. (1957). "The construction of a SEM and its application to the study of fibres," Ph.D. Dissertation, Cambridge University.
Wells, O. C. and Bremer, C. G. (1968). "Voltage measurement in the scanning electron microscope," J. Phys. E **1**, 902–906.
Wells, O. C. (1971). "Low-loss image for surface scanning electron microscope," Appl. Phys. Lett. **19**, 232–235.
Wells, O. C. (1974). *Scanning Electron Microscopy* (McGraw-Hill, New York).
Wells, O. C. (1978). "Penetration effect at sharp edges in the SEM," Scanning **1**, 58–62.
Wells, O. C., Savory, R. J. and Bailey, P. J. (1982). "Backscattered electron (BSE) imaging in the scanning electron microscope (SEM)—measurement of surface layer mass-thickness," Proceedings of Asilomar Conference, 1982 (in press).
Whetten, N. R. (1961). "A review of experimental methods in the field of secondary electron emission," General Electric Res. Lab. Rep. No. 61-RL-2733 E.
Willis, R. F. and Feuerbach, B. (1975). "Angular-resolved secondary electron emission spectroscopy of clean and adsorbate covered tungsten single crystal surfaces," Surf. Sci. **53**, 144–155.
Wittry, D. B. (1966). "Secondary electron emission in the electron probe," *Optique de rayon X et microanalyse*, edited by Castaing, Descamps, and Philibert (Herrmann, Paris), pp. 168–188.
Young, J. R. (1956). "Penetration of electrons in $Al_2O_3$-films," Phys. Rev. **103**, 292–293.
Young, J. R. (1957). "Dissipation of energy by 2.5–10 keV electrons in $Al_2O_3$," J. Appl. Phys. **28**, 524–530.



Downloaded 28 Jan 2009 to 146.137.148.78. Redistribution subject to AIP license or copyright; see http://jap.aip.org/jap/copyright.jsp